An Approach to Quantifying Uncertainty in Estimates of Intensity Duration Frequency (IDF) Curves

by

Fahad Alzahrani

A thesis
presented to the University of Waterloo
in fulfillment of the
thesis requirement for the degree of
Master of Applied Science
in
Civil Engineering

Waterloo, Ontario, Canada, 2013

AUTHOR'S DECLARATION

I hereby declare that I am the sole author of this thesis. This is a true copy of the thesis, including any required final revisions, as accepted by my examiners.

I understand that my thesis may be made electronically available to the public.

Abstract

Generally urban drainage systems are built to protect urban property and control runoff. Moreover, these systems collect the runoff for storage purposes to serve society through sufficient water supply to meet the needs of demand, irrigation, and drainage. Urban environments are exposed to risks of extreme hydrological events. Therefore, urban water systems and their management are critical. Precipitation data are crucial, but may be prone to errors due to the lack of information e.g., short length of records. In this thesis, a Monte Carlo simulation and regional frequency analysis based on L-moments approach were utilized during the research in order to estimate the uncertainty in the Intensity Duration Frequency (IDF) curves by using historical precipitation data from Environment Canada (EC) weather stations and simulating a new series of data through a weather generator (WG) model. The simulations were then disaggregated from daily into hourly data for extraction of the annual maximum precipitation for different durations in hours (1, 2, 6, 10, 12, and 24). Regional frequency analysis was used to form the sites into groups based on homogeneity test results, and the quantile values were computed for various sites and durations with the return periods (T) in years (2, 10, 20, and 100). As a result, the regional frequency analysis was used to estimate the regional quantile values based on L-moment approach. Moreover, the box and whisker plots were utilized to display the results. When the return periods and durations increased, the uncertainty slightly increased. The historical IDF curves of London site falls within the regional simulated IDF curves. Furthermore, 1000 runs have been generated by using the weather generator.

Acknowledgements

All praises are due to Allah for giving me the ability to write this work. All praises are due to Allah for giving me the honor of helping humanity by contributing to the enrichment of knowledge.

I would like to thank my supervisor, Dr. Donald H. Burn, for his guidance and support throughout the completion of my Master's degree. I cannot thank him enough for his thoughtful guidance, generous support, and friendly discussions which helped me to improve my academic knowledge. I would also like to thank the committee members for their valuable suggestions and feedback they provided for this thesis. Finally, I would like to thank my family, friends, and fellow graduate students who have supported me throughout the completion of my Master's degree. I would especially like to thank my parents, Saeed and Shamsah, for their support over the years, and my wife, Ahlam, for her patience and encouragement. I would like to acknowledge the support of Saudi Cultural Bureau in Ottawa, Ontario, and King AbdulAziz University, in Jeddah, Saudi Arabia for their generous funding.

Table of Contents

List of Figures

List of Tables

Chapter 1: Introduction

1.1 Background

Urban environments are exposed to the risk of extreme hydrological events. Therefore, urban water systems (including culverts, storm water ponds, creeks, drainage systems, and storm sewer systems) along with infrastructure design and management are critical to lessen the risk of flooding. Intensity-Duration-Frequency (IDF) curves can be obtained based on historical data and are usually employed to evaluate the extreme values of precipitation in urban drainage systems. For instance, IDF curve estimates are crucial in urban drainage systems so as to have a consistent estimation of extreme precipitation to design the conveying and detention infrastructures. Therefore, IDF curves can be defined as mathematical tools that express the relation between intensity, duration, and return period of precipitation. Three stages used to obtain the IDF curves are extraction of annual maximum precipitation, fitting distribution in each maximum time series, and estimation of IDF curve parameters. One challenge in determining extreme precipitation events is the issue of uncertainty. Sources of uncertainty include inadequate data records as well as parameter and model uncertainty (Elsebaie, 2011; Xu et al., 2010; Sharif & Burn, 2007). Hailegeorgis and Burn (2009) identify several additional potential sources of uncertainty, which are detailed in Chapter 2. This thesis will undertake simulations and statistical analysis to quantify the uncertainty in IDF curve estimates.

A source of uncertainty could be the IDF characteristic of data length. This could affect the uncertainty on the IDF curve which could lead to greater risk and require decisions in order to find the proper design and cost of hydraulic structures. This emerging uncertainty is due to lack of precipitation data, and is a major concern with water resources management. Thus, in this thesis, regional frequency analysis approach has been used to coordinate data series. Homogenous regions have been identified from several sites to generate regional frequency curve.

There are different methods used to quantify the uncertainty in IDF curves, such as Monte Carlo Simulation (MCS), Kernel estimators, Bayesian estimations, and Fuzzy Alpha Cut Logic. In this research, MCS - a common stochastic model - was used to estimate the uncertainty in IDF curves. MCS is involved in two processes: defining an input domain and generating random inputs from a probability distribution over the domain.

In water resources management and planning, assessment of uncertainty in IDF curves must be considered in terms of economics and the environment. Essentially, urban water systems protect urban property by controlling the runoff. However, if IDF curves were inaccurately estimated and the urban water system was designed improperly, the urban area would be at high potential risk of flooding (Figures 1-1, 1-2).

Figure 1-1 Flood in the canal of King Abdullah Road, Jeddah, Saudi Arabia, November 2009.

Figure 1-2 Flood in Makkah road, Jeddah, Saudi Arabia, November 2009.

1.2 Objectives of the thesis

The thesis, which is motivated by observed and modeled storm design, quantifies the uncertainty of precipitation events. Therefore, the main goals are to quantify the uncertainty in IDF curves using Monte Carlo simulation method, and increase the understanding and knowledge of precipitation events in spite of uncertainties.

1.3 Organization of the thesis

The remainder of the thesis is organized as follows. Chapter 2 provides a literature review of

material relevant to the subject, and includes four sections. Chapter 3 presents an overview of the methodology used during this research. Chapter 4 discusses background information about the case study application, the Upper Thames River in London Ontario, along with the results and discussion. Finally, Chapter 5 concludes this project and suggests future work.

Chapter 2: Literature Review

2.1 Introduction

The scope of this chapter focuses on how researchers have identified, estimated, and assessed uncertainty on any aspect of hydrology using Intensity Duration Frequency (IDF) curves. Furthermore, the literature review will focus on the following topics: regional frequency analysis, uncertainty analysis method, and IDF curves.

Related research about uncertainty in IDF curves depends upon stochastic analysis and numerical simulation from observed data. Similarly, changes in climate and environment can also contain uncertainty. Overall, it is clear that uncertainty assessments aid researchers in the field of water resources management and hydraulic structures to design proper urban systems by relying on statistics and engineering concepts that prevent and control floods and reduce the loss of life, property, and surface pollution. Therefore, the estimation of uncertainties depends upon the sources that cause them, and is based on stochastic simulations and comparisons between the parameters of simulated samples (distribution probabilities parameters).

2.2 Regional frequency analysis

Frequency analysis is defined as the estimation of how likely it is that an event will occur. Regional frequency analysis estimates the frequency distribution of observed data for each site using collected data from several sites (Hosking & Wallis, 1993). The principles of regional frequency analysis apply whenever there are multiple samples of similar data. Therefore, the aim of frequency analysis is to obtain the valuable estimation of the quantile values for a return period. In hydrology, regional frequency analysis has been established over the last decades. The

index-flood is an early example (Dalrymple, 1960). National organizations like the U.S. Water Resources Council (1976) through Bulletin 17 recommended several methods for general use by hydrologists such as fitting a log Pearson type III distribution to annual maximum stream discharge at a single site. Regional frequency analysis depends on the index storm approach, which is widely used in precipitation events quantile estimation (Hosking & Wallis, 1997). However, additional information from sites through the region is applied at site assessments to obtain estimations for sites without observations. Hosking and Wallis (1997) indicated that each step for regional frequency analysis depends on the previous steps. In total, there are four main steps in regional frequency analysis: screening the data, homogeneous regions identification, deciding upon frequency distribution, and estimation of frequency distribution. Regional frequency analysis of precipitation events requires the availability of precipitation data at sites of interest. Martins and Stedinger (2002), Lin and Chen (2006), and Burn (2003) have demonstrated the importance of using regional frequency analysis for extreme hydrological events.

L-moment approach can be used under regional frequency analysis. For example, the L-moment describes the shape and location of data series in the distribution, and briefly outlines the statistics of probability distributions and data samples (Hosking & Wallis, 1997). For data samples, Greenwood et al. (1979) have stated that probability-weighted moments are precursors or leaders of the L-moments. Therefore, the sample probability weighted moments are computed from data values X_1, X_2, ... X_n, arranged in increasing order, as given in the following equation:

$$b_o = n^{-1} \sum_{j=1}^{n} X_j \qquad \text{Eq (2.1)}$$

$$b_r = n^{-1} \sum_{j=r+1}^{n} \frac{(j-1)(j-2)\ldots(j-r)}{(n-1)(n-2)\ldots(n-r)} X_j \qquad \text{Eq (2.2)}$$

where b_0 and b_r are unbiased estimators of the probability weighted moment. Basically, L-moments are linear combinations of probability-weighted moments, and their probability weighted moments are defined by Greenwood et al. (1979) to be the quantities:

$$M_{p,r,s} = E\{X^p[F(X)]^r[1-F(X)]^S\} \qquad \text{Eq (2.3)}$$

$$\beta_r = M_{1,r,0} = E\{X[F(X)]^r\} \qquad \text{Eq (2.4)}$$

where $p, r,$ and s are the non-negative integers. The conventional moment of order p is represented by $M_{p,r,s}$. The probability-weighted moments are difficult to explicate directly as the probability scale and shape. The first L-moment describes the mean of data sample and the second L-moment describes the dispersion of the data values (Hosking & Wallis, 1997). The regional frequency analysis based on the L-moment approach has been found practical for confirming both differences and similarities (Eslamian & Feizi, 2006). Therefore, the goal is to demonstrate the results by identifying the goodness of fit measures and estimating the distribution's parameters (Hosking & Wallis, 1991). This approach is usually applied when determining the parameters and suitable distribution. Eslamian and Feizi (2006) have applied regional frequency analysis based on L-moment approach on Iranian rainfall data. Their results found that the homogeneity and similarity tests are reliable for overcoming problems caused by short length data. In addition, the L-moment has been widely used in most recent studies, especially studies of hydrological events. For instance, Dodangeh et al. (2011) used L-moments analysis of dust frequencies in Iran, and concluded that the distributions with the best fit to the data grouped sites are generalized normal, generalized Pareto, and Pearson type III. The L-moment method was used in another study by Markus et al. (2007) which concluded that the

average design precipitation for 12 stations located in Illinois is larger than TP-40 results (TP-40 is a technical paper completed by US Weather Bureau). The researchers used the L-moment method for evaluating storm design and comparing the output with other sources.

Finally, the L-moment is an approach used in regional frequency analysis that describes the statistical properties for any data series. This analysis aids in determining the quantiles values; moreover, these values can be used to estimate the probability of the storm events. The results of this review indicate that many researchers are dependent on this approach, which suggest its potential effectiveness in estimating uncertainty in further studies. The L-moment approach is also useful in designing projects related to water resources management.

2.2.1 Data screening

Data screening is defined as the process of inspecting data for errors and correcting them prior to data analysis. The screening may involve checking raw data, identifying outliers, and dealing with missing data. Data screening is clearly a significant aspect of the regional frequency analysis process; thus, gross errors and inconsistencies need to be removed before applying the data analysis. Overall, data screening is divided into two main sources of error which are derived from measurement errors and errors in the data collected under climate conditions.

The circumstances of data collection may be affected over time. For example, a station's device may change location. A study by Wallis et al. (1990) compiled a set of daily precipitation records supplied by National Climate Data Centre (NCDC) for 1009 sites located in the United States. Although precipitation daily data were collected from original sources and underwent

validity preprocessing for incorporation of historical data, at least 38 percent of the sites had gross errors such as daily precipitation less than zero.

There are at least three useful methods of checking data in regional frequency analysis. First, according to Wallis et al. (1990), checking individual data values can potentially disclose gross errors. Second, separately checking the site's data can differentiate isolated values and iterated values that may arise from errors in the recording data (Hosking & Wallis, 1997). Third, comparing the L-moment ratios of samples for different sites can decide whether sites are discordant or not.

Finally, data screening is an essential process for regional frequency analysis. This process identifies and corrects the gross errors in the data. In addition, the L-moments ratios have been found useful for the screening of the data for sites by using a discordancy measure.

2.2.2 Homogenous group delineation

The aim of homogeneous group delineation is to form homogenous groups of sites in order to measure the homogenous values. This process is usually difficult and requires subjective judgment. Hosking and Wallis (1997) identified a method for homogeneous regions delineations called grouping methods. Grouping methods, which have been proposed by several authors for forming a group of similar sites, include geographical convenience, subjective and objective partitioning, and cluster analysis. Pooled frequency analysis of precipitation uses local observations at gauged sites for quantile estimation. The delineation of homogenous areas is an essential task of regional frequency analysis, as proper delineation is crucial in the reliable estimation of quantile (Castellarin et al, 2008). The sites must be designated to homogeneous

regions in order to process the regional frequency analysis. Clearly, approximate homogeneity is desired when ensuring that regional frequency analysis is more constant than at-site analysis (Hosking & Wallis 1997; Lin & Chen 2003). Thus, when many sites are included in regional frequency analysis, identification of homogeneous regions is often a difficult stage which requires a certain amount of judgment by individual researchers (Lin & Chen, 2006). In the identification of homogeneous groups, similar sites correspond to the region.

This section will summarize the most common approaches that are employed in homogenous group delineation. One common procedure in hydrology for delineation of similar sites in a region is region of influence (ROI) approach (Burn, 1990). This method is used for the target site of interest based on the pooling group. Therefore, this approach has an advantage of decreasing the heterogeneity in the choosing of similar sites. The group homogeneity and its target size dominate the effective identification of the pooling group (Burn et al., 2000). In the region of influence approach, the homogeneity similarity group is determined based on the climate or meteorological information corresponding to the observation stations; therefore, a weighted and scaled Euclidian distance metric in P-dimensional space measures the similarity among sites and is defined by sets of catchments' characteristics e.g., flow, precipitation, and length (Burn et al., 2000). The dissimilarity between other sites will be determined using the following equation:

$$d_{i,j} = \sqrt{\sum_{k=1}^{P} w_k \left(\frac{x_k^i - x_k^j}{S_k}\right)^2} \qquad \text{Eq (2.5)}$$

Where

$d_{i,j}$ is the distance metric between site i and site j, w_k is the weight applied to attribute k reflecting the importance of the attribute with respect to the others, x_k^i and x_k^j are the values of the k^{th} attribute for sites i and j respectively, and S_k is the sample standard deviation of the k^{th} attribute and P-dimensional space. Cluster analysis, which is a standard approach of statistical multivariate analysis to divide the data into groups, has been successfully used for forming the region for regional frequency analysis. De Coursey (1973) used the cluster analysis approach to form the streamflow characteristics sites due to their similar flood response. For the purpose of regional frequency analysis, Burn (1989) used cluster analysis to divide the flood data to regions. The formation of data series depends on statistical properties or geographical convenience. The artificial neural networks are currently used to deal with a large amount of data series; therefore, different kinds of artificial neural networks are categorized by their network structure (Lin & Chen, 2006). Lin and Chen (2006) have applied the artificial neural networks' self-organization map to identify the homogenous group for regional frequency analysis.

In summary, homogenous group delineation (e.g., ROI, cluster analysis, and artificial neural networks) has been widely used in the peer-reviewed literature to analyze hydrological events.

2.2.3 Homogeneity tests

The homogeneity examination is a frequently used test for regional frequency analysis and is a significant component of numerous regional flood frequency analysis methods (Fill & Stedinger, 1995). Hosking and Wallis (1997) indicated sampling from the four parameter Kappa distribution and the three heterogeneity measures were used to examine the variability of three

different L-statistics: H_1 for coefficient of L-variation (L-CV), H_2 for the combination of L-CV and L-skewness (L-SK), and H_3 for the combination of L-skewness and L-kurtosis (L-CK). In the observed data and simulated regions, the H_1 values were more powerful than the other heterogeneity measures of H_2 and H_3 statistics (Hosking & Wallis, 1997). In the following formula proposed by Hosking and Wallis (1997), heterogeneity measures (H) statistics are computed as:

$$H_i = \frac{V_{obs_i} - \mu_{V_i}}{\sigma_{Vi}}, i = 1, 2, 3, \ldots \ldots \quad \text{Eq (2.6)}$$

where $\mu_{V_i}$and σ_{Vi} are the means and standard deviations of the simulated values of dispersions (V_i) while V_{obs} is the regional dispersion calculated from the regional observations. Hosking and Wallis (1997) suggested that a region can be regarded as "acceptably homogeneous" if H < 1, "possibly heterogeneous" if 1 ≤ H < 2, and "definitely heterogeneous" if H ≥ 2. These Hosking and Wallis measure tests (Viglione et al., 2007) are an accurate examination of homogenous-pooled delineation when the L-SK is low. Viglione et al. (2007) completed a comparison in regional frequency analysis by using three different tests. One test was based on the L-moment approach, which is more powerful when samples are positively or negatively skewed. Based on these findings, Viglione et al. (2007) advised a straightforward methodology to lead the homogeneity test choice in order to be useful for various possible cases. The researchers counsel the kappa distribution parameters to make the group of flood sequences and prevent any problem of excessive obligation to a specific three parameters distribution (Hosking & Wallis, 1997). All studies mentioned in this review chose the Hosking and Wallis homogeneity test because of its accurate values and dependability. In addition, by using the equations that are expressed above, it

is possible to delineate the homogeneous level into groups or regions. In summary, this process (homogeneity test) is one of the regional frequency analysis processes proposed by Hosking and Wallis (1997).

Another homogeneity test is the bootstrap Anderson-Darling (AD) test, which does not assume the distribution. Instead, the AD test generalizes the classical Anderson-Darling goodness of fit test by evaluating the hypothesis that independent samples pertain to the same population without determining their distribution function (Scholz & Stephens, 1987; D'Agostino & Stephens, 1986).

After the homogeneity tests, the quantile estimation will be determined. The steps of the quantile estimates are part of L-moment processes. The probability distribution parameters for each homogenous site were computed and determined by L-moments as defined by Hosking and Wallis (1997). The following equation (Eq 2.7) is the inverse function that can be expressed in dimensionless form.

$$\hat{Q}_i(F) = \mu_i q(F) \qquad \text{Eq (2.7)}$$

where the $\hat{Q}_i(F)$ is quantile function for station i, μ_i is the mean of station and $q(F)$ is the regional growth curve. The quantile estimates for annual precipitation were computed by multiplying the regional growth curve by the at-site value of annual precipitation (Hosking & Wallis, 1997).

2.3 Uncertainty assessment methods

Uncertainty occurs in any environmental phenomena because of the behaviour of humans and nature, such as climate change or global warming (Guo, 1995). Because of these reasons,

there are uncertainties in hydrologic climatic data. In the following reviews, the uncertainty assessment will be indicated. Uncertainty is associated with data components, noise in the incomplete data, and random sampling errors. In addition, problems with models can be considered a source of uncertainty, such as an error in a model's structure (Moss & Schneider, 2000). Due to human behaviour, uncertainty can occur because of future consumption patterns such as water consumption (Moss & Schneider, 2000). A study by Xu et al. (2010) classified the uncertainty into data uncertainty and model uncertainty. Based on these classifications, the sources of uncertainties could be established through modeling extreme hydrologic events, as shown in Figure 2-1 (Xu et al., 2010). Furthermore, it was concluded that uncertainty is high in extreme rainfall/runoff quantile estimation (Xu et al., 2010). Uncertainty assessment methods are many, and are primarily based on the condition of data. For example, estimating uncertainties in water resources can be assessed using various methods such as Monte Carlo Simulation experiment, Fuzzy-Logic approaches, and Bayesian model averaging.

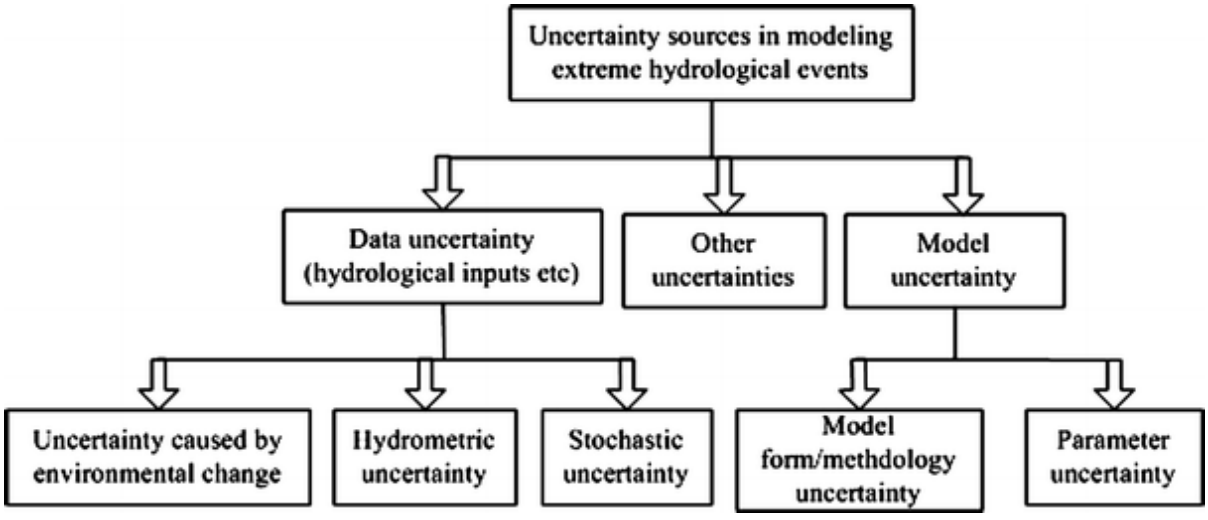

Figure 2-1 Classification of uncertainty sources in modeling extreme hydrological events (Xu et al., 2010)

Based on several assumptions in estimating uncertainty in precipitation (e.g., variance in measurement period between weather stations), two approaches are fundamentally applied for uncertainty assessment: Bayesian statistics approach and Kernel density estimation (Soliman, 2011). The first method is used to determine a distribution from the past observed data, as developed by Tebaldi et al. (2005). It contains a Bayesian implementation and reliability ensemble averaging approach extension (Giorgi & Mearns, 2003). The second method is used to estimate and quantify the uncertainties in results, and is defined as a non-parametric way to estimate the probability density function of the random variable (Soliman, 2011). This method is widely used as an acceptable and flexible alternative to parametric methods in the hydrology field (Sharma et al., 1997). There are several methods for estimating the uncertainty. Each method has a different approach towards stochastic simulations.

2.3.1 Monte Carlo simulation method (MCS)

Monte Carlo simulation method is defined as a stochastic method that repeats a sample of random variables from specific probability distribution in order to measure the reaction of the stochastic system (Hailegeorgis & Burn, 2009). Prudehomme et al. (2003) have relied on this methodology in order to quantify the uncertainty of climate change on flood regime in UK small catchments areas.

The appropriate probability must be determined for each uncertain input of the model. Therefore, the probability choice has a direct impact on the computed results. Monte Carlo simulation contains several steps: 1) drawing the random sample for each random variable from its statistical distribution; 2) evaluating the model; 3) counting the results; 4) analyzing the

results using statistics, histogram, and confidence intervals; and 5) transmitting the input parameters to the model predictions.

Monte Carlo simulation has been shown to be the most effective method of studying uncertainty in parameters of depth, duration and return period (Melching et al., 1990), because the simulations allow for the generating of many samples. The study by Harlin et al. (1992) is in agreement with the study of Melching et al. (1990) in that this simulation is effective for uncertainty assessment. In another uncertainty assessment study completed by Guo and Ying (1997), Monte Carlo simulation (1000 runs simulation) was used and applied to estimate uncertainty in IDF parameters in two case studies located in China. Similarly, the authors concluded that uncertainties in model parameters and runoff are huge when the runoff coefficient of the basin is small. Monte Carlo method was also used by Drees and Kaufmann (1998) in order to estimate the optimum fractions of data to assess the Hill estimator for extreme value index. As shown in Figure 2.1, the uncertainties have been classified depending on their sources in hydrological modeling (Xu et al., 2010).

2.3.2 Fuzzy set theory

A fuzzy class is identified by the membership function that is associated with a real number in the interval between 0 and 1 (Zadeh, 1965). The membership function includes the whole fuzziness for a specific fuzzy class, and is described as the fuzzy operation quintessence (Zadeh, 1965; Ross, 2004; Vucetic and Simonovic, 2011). The fuzzy set theory has been developed to capture a judgmental belief, as the uncertainty is usually caused by lack of information (Vucetic and Simonovic, 2011). An object within the fuzzy set is marked in the interval between 0 and 1.

The fuzzy class measures the degree that an event occurs; therefore, the fuzzy set shows whether the event has occurred or not (Vucetic and Simonovic, 2011). In general, applying the fuzzy theory could successfully quantify the uncertainty and represent the sources of the uncertainty (Vucetic and Simonovic, 2011).

Vucetic and Simonovic (2011) have quantified the uncertainty faced by water resources management decision makers by using fuzzy theory and probabilistic approach. Notably, water resources decision makers are exposed to several sources of uncertainty that might compromise the ability to make effective decisions. The authors' goal was to illustrate how information provided to water resources decision makers can be improved by using the tools that incorporate uncertainty. As a result, the study concluded that fuzzy theory and probabilistic approach could accurately quantify the uncertainty.

Shrestha and Simonovic (2009) have used the fuzzy set theory as a methodology to represent individual sources of uncertainty in the stage and discharge measurements and their aggregation into the combined uncertainty. As a result of their study, the authors concluded that fuzzy set theory provides a proper methodology for uncertainty analysis.

In conclusion, these two studies have shown that the fuzzy set theory can be used effectively for uncertainty quantification. Specifically, the fuzzy set theory can be used for water resources management decision making as well as for determining the sources of uncertainty.

2.4 Intensity duration frequency (IDF) curves

2.4.1 IDF estimation methods for single site, pooled data

IDF curves are used in combination with runoff estimation formulas such, as the rational method, in order to predict the peak runoff flow from exact point of basin. These are also used in certain aspects of hydraulic structures design such as size of pipes and culvert (Dupont & Allen, 2000). Further research has used the IDF curves for different areas (Ilona & Frances, 2002).

IDF curves are the relationship between the return periods, depth, and duration; these curves are also generated in order to determine the extreme characters of precipitation in urban drainage and hydrology. In urban water system design, IDF curves are particularly pertinent in considering the estimations of IDF curves to design conveying and detention infrastructure in an ideal path. If the estimations of these extremes are computed incorrectly, the results may indicate an unacceptable risk of flooding and property loss. Their estimations must be determined carefully, because any failure in computation and design will have costly consequences for water resources engineers. There are two current approaches which model extreme precipitation: annual maximum series (AMS) and Bayesian estimation for IDF (Coles, 2001). The AMS could be modeled by using probability distributions such as Gumbel distribution and generalized Pareto distribution (Katz et al., 2002).

Bayesian and classical IDF curves are similar methods of computing the IDF values, and the classical estimation estimates the parameter distribution is commonly used. The following are classical estimation methods for IDF curves: method of L-moments, method of maximum likelihood, and method of probability weighted moments (Hurad et al., 2010). The maximum

likelihood method has been most efficient for long return periods and moderate sample sizes (Madsen et al., 1997). Hurad et al. (2010) concluded the Bayesian estimations for IDF curves are much better than classical estimations, and suggested using the Bayesian analysis rather than using the classical method to incorporate parameter uncertainty in computing the IDF curves and estimating the return periods.

Al-Dokhayel's (1986) study used two continuous probability distributions to estimate the rainfall depth frequency relationships with various return periods for Qassim region, Saudi Arabia, the distributions are the extreme value type I distribution (Gumbel max distribution, which is commonly used in hydrology fields), and Log Pearson distribution Type III (LPT). In addition, remote sensing and satellite data are new technologies for determining and developing the IDF curves (Elsebaie, 2011). A study conducted by Awadallah et al. (2011) developed the IDF curves for short length data by using regional analysis, and presented a methodology used to overcome the lack of precipitation data by joining the ground data with TRMM satellite and developing the ratios between 24 hours precipitation depth and short duration depths. Similarly, Alhassoun (2011) developed the empirical formula which helps estimate the rainfall intensity for a region, and concluded that there were no differences in rainfall analysis results between Gumbel max and LPT methods. These reviews indicate the significant role of IDF curves in hydraulic structures design.

Developing the IDF curves requires reliable precipitation intensity that is necessary for accurate hydrological analyses (Elsebaie, 2011). Elsebaie (2011) utilized two methods to estimate the rainfall intensity and develop the IDF curves. As a result, the Gumbel max and LPT

distributions results are close. It is clear that these techniques indicate agreement in the results of recent research. Furthermore, these results agree with Bayesian estimation for IDF curves by using prior distribution. Below is the most common empirical formula for determining the intensity (I):

$$I=\frac{a}{(d+b)^e} \qquad \text{Eq (2.8)}$$

Where I is intensity of the precipitation (mm/hr), a, b, d and e are parameters.

Return period can be estimated based on the probability density function with quantiles. In the mathematical approach, Coles et al. (2003) suggest that return period could be computed by using the Markov Chain Monte-Carlo sampling (MCMC). The return period is calculated by the two following sets: drawing the set of GEV parameters θ from posterior distribution parameters by Monte Carlo sampling $f(\theta|x)$, and computing T_e from the equation below for each $\theta \; and \; x$. Where x is a sample value and the $F(e|\theta)$is the inverse of the probability function.

$$T_e = \frac{1}{(1-F(e|\theta))} \qquad \text{Eq (2.9)}$$

This formula determines the return period (T). Hurad et al. (2010) estimated the return period and concluded that the return period estimations are very sensitive to assumptions about the event because the return period is used to compute the probability of event occurrence (e.g., storm).

To conclude, the IDF curves are determined by using the inverse probability distribution function. Quantile values can be obtained by the inverse probability distribution function; these indicate the return level that is expected to exceed every time interval and return period. In

addition, the IDF curves can be determined and constructed by using several distributions such as Gumbel max value distribution.

2.5 Conclusions

This chapter has reviewed research relevant to the subject of quantifying an approach of uncertainty estimates on the IDF curves. Several relevant aspects have been presented in this chapter, including regional frequency analysis process, uncertainty assessments, and IDF estimations. Furthermore, the reviews have estimated the uncertainty by using different models that consider the impact of climate change. Overall, these reviews have found uncertainty estimates on IDF curves to be most beneficial. Studies have indicated that regional frequency analysis based on the L-moment algorithms is a powerful method helpful for short data records. In addition, the identification of a homogenous group is an extremely valuable process that facilitates the forming of data records. After reviewing the literature on quantifying an approach of uncertainty estimates on the IDF curves, this research will quantify the uncertainty in IDF curves by using the approaches mentioned in the literature to solely focus on the precipitation without including the impact of climate change.

Chapter 3: Methodology

3.1 Introduction

The goal of the thesis is to estimate the uncertainties in Intensity Duration Frequency (IDF) curves. Sources of uncertainties may be associated with data errors e.g. short records of data. This chapter will explain the methodologies used throughout this project, including weather generator (WG), disaggregation approach model, extraction of annual maximum precipitation, and regional frequency analysis. The uncertainty development includes the following steps:

1. Set up the input data - historical data are assembled from climate stations, including data for different climate variables.
2. Run the WG model to produce new sequences of precipitation data.
3. Run the disaggregation model to obtain the hourly series.
4. Extract the annual maximum precipitation. Annual maximum precipitation is extracted for each station and each year for the duration of 1 hour, 2, 6, 12, and 24 hours.
5. Estimate the extreme precipitation quantiles. The quantile values are computed by using regional frequency analysis based on L-moment algorithms.
    a. Homogeneity test
    b. Fitting the data into a probability distribution
    c. Estimating the quantile values

Each step depends on the previous step, and needs to be repeated several times to estimate the uncertainty. Development and estimation of uncertainties will be further elaborated on within this chapter.

WG has been developed to generate simulated precipitation data; this includes meteorological data that are used as input in the model. The disaggregation model is a statistical approach that classifies the data into different parts or forms. Therefore, WG results are used as input through the disaggregation model to provide the simulated hourly data based on hourly historical data. Finally, to generate the IDF values, three models common in statistical field have been used: weather generator model, disaggregation model, and Hosking &Wallis model.

3.2 Weather generator model

In hydrology and water resources management, the weather generator model has an important task. Weather generator (WG) is defined as a stochastic model that produces a simulated series of unlimited length of data, usually by inputting observed weather data to produce the simulated weather data. Improved K-nearest neighbor (KNN) weather generator model is used as a tool in this research (Sharif & Burn, 2007). In addition, the input data to the model is the daily observed precipitation, and the output from the model is the simulated daily precipitation. The model generates a realistic output series, and KNN allows reshuffling of the input data series (Sharif & Burn, 2007). The aim of using WG in this research is to obtain the output sequences and use them in the disaggregation model.

3.3 Creating simulated hourly precipitation using disaggregation model

The disaggregation model is a deterministic model that extracts a component of data series into a number of parts e.g., this model is disaggregating the daily simulated data into hourly simulated data. In this thesis, WG is used to create climate values on daily series; therefore, the disaggregation model's mechanism has been developed to produce a time series of hourly precipitation data. This model is completed based on the fragments method (Svanidze, 1977; Sharif et al., 2007). The fragments represent the daily precipitation fraction, which occurs hourly. The following equation expresses the fragments for each day based on measured data:

$$f_i = \frac{h_i}{\sum_{i=1}^{n} h_i} \qquad \text{Eq (3.1)}$$

Where f_i represents the fragments computed per hour i; h_i is the chosen historical hourly data, and n represents the number of hours per day (24 hours). Then, the fragments are multiplied with the daily data from weather generator to create hourly data:

$$h'_i = f_i \times d \qquad \text{Eq (3.2)}$$

Where d is daily precipitation in (mm), and h'_i is the new hourly simulated precipitation (mm). Results have been compared in an attempt to verify that the model is working correctly, and avoid any error in output. This approach (using disaggregation model) employs locally observed data by using the non-parametric method to avoid the chance of errors, which might occur from parametric methods because of theoretical distribution fits and parameter estimations e.g. short length of data series and errors in reading of data series.

To compute the hourly value of each day, the disaggregation model was used to determine the hourly information for each day of precipitation and to enable the extraction of the annual

maximum values for different durations in hours. Therefore, the scheme of disaggregation model works by extracting precipitation events from hourly-observed data. A precipitation event is defined as a non-zero precipitation period. Once the precipitation events are extracted, they are disaggregated by K-NN approach. The model works by comparing a number of days to the current day of precipitation event; hence, the best match is estimated by the following formula (Mansour & Burn, 2010):

$$Z_i = \sqrt{(w_1 * (y_i - x_i)^2) + (w_2 * \left(e_y - e_x\right)^2)} \qquad \text{Eq (3.3)}$$

where y_i is the new daily precipitation from WG, x_i is the historical daily precipitation,and e_y and e_x are events that are computed from WG outputs and historical data respectively. The weights (w_1, w_2) values are used to decide which historical hourly ratio is the best for the data series. The hourly value set within the moving window of days could be chosen for same events (w_2) or the total daily precipitation (w_1). The value (Z_i) found in the window that is chosen to be the daily ratio of historical hourly values is used to transfer the WG output daily data into hourly values. However, the hourly ratio values found within the chosen day are then applied to the daily value to create a probable hourly data for the given daily data. This program is sent daily data including known hourly values, and the results have been compared to verify the model is working properly (for further details see Sharif and Burn, 2007; Solaiman, 2011).

3.4 Determining the annual maximum precipitation

Annual maximum precipitation means a maximum event that has occurred annually for various durations of the event e.g. 1 hour, 2, 6, 12, 24 hours. After running weather generator and

disaggregation model, the next step is determining annual maximum precipitation for hourly durations of 1, 2, 6, 12, and 24 for the purpose of estimating the quantile values. The mechanism of this calculation occurs over every single hour through the entire series of data to determine the maximum precipitation for one hour duration and every two hours to determine the maximum precipitation for two hours duration, and continues in this way for every six hours, 12 hours, and 24 hours. These steps should be completed for all stations, as annual maximum results are very important for regional frequency analysis process.

3.5 Estimating the extreme precipitation quantile values

3.5.1 Quantile estimation for single site

A quantile describes location of values in a probability distribution. Pearson type III distribution is used to estimate quantile values for historical single site data (London site), because the single site data are in range skewness coefficient between -9 and 9, and this distribution is widely recommended in water resources fields. In the following formula, the Probability Density Function (PDF) of the Pearson type III distribution (P3) is:

$$f(y) = \frac{|\beta|}{\Gamma(\lambda)}[\beta(y-m)]^{\lambda-1}e^{-\beta(y-m)} \qquad \text{Eq (3.6)}$$

Where m and λ, β are parameters and (y) is a random variable. There is no explicit formula for the inverse of Pearson type III distribution; therefore, many researchers have developed approximate formula inverse of Pearson type III distribution formula (Vogel & McMartin, 1991). Chowdhury and Stedinger (1991) have compared five approximations to frequency factor (K_i). The authors found the inverse of standardize Pearson type III distribution random variables where:

$$M_i = \mu + \sigma K_i \quad \text{Eq (3.7)}$$

Where μ is the mean and σ is the standard deviation as cited in Vogel & McMartin (1991). The inverse of Pearson type III distribution contains four parameters and the inverse of standard normal distribution function, where *Ki* is the frequency factor as expressed in the following formula:

$$K_i = A\left\{\{max\left[D, 1 - \left(\frac{B}{6}\right)^2 + \left(\frac{B}{6}\right)\phi^{-1}(p_i)\right]^3 - C\right\} \quad \text{Eq (3.8)}$$

Where

$$A = \max(\frac{2}{\gamma}, 0.40) \quad \text{Eq (3.9)}$$

$$B = \gamma - 0.063 \max(0, \gamma - 1)^{1.85} \quad \text{Eq (3.10)}$$

$$C = 1 + 0.0144 \max(0, \gamma - 2.25)^2 \quad \text{Eq (3.11)}$$

$$D = \left\{C - [\frac{\frac{2}{\gamma}}{A}]\right\}^{1/3} \quad \text{Eq (3.12)}$$

$\Phi^{-1}(p_i)$ is a standard normal distribution function inverse, p_i is the selected probability level, and *A*, *B*, *C*, *D* are the parameters. These formulas have been applied for historical single site in order to estimate the IDF values (M_i).

3.5.2 Homogeneity tests

Sites are located within 50 km of each other, and are sorted based on the distance between sites in kilometers. The homogeneity test is used based on the L-moments approach. The homogeneity is used to estimate the *H* values, the whole sites are involved in the homogeneity measures for different durations, and the homogeneity test is applied to historical data in order to

decide the group number of sites. By choosing the number of group sites, the regional quantile value is easily estimated.

The homogeneity test is a step of regional frequency analysis used to determine the number of pooled sites. To apply the regional frequency analysis and quantify the uncertainty in IDF curves, the data sites are sorted in ascending order from central site based on the distance between sites in km. Next, the homogeneity test is applied. Due to sensitivity in this process, sites are sorted into groups starting with 2, 3, 4, up until 9 sites for all durations in hours. As a result, homogenous values are found.

To review what presented in chapter 2, the homogeneity measure is then expressed as:

$$H = \frac{V - \mu_v}{\sigma_v} \qquad \text{Eq (3.4)}$$

According to Hosking and Wallis (1993), a region can be declared homogeneous if $H < 1$, possibly homogeneous if $1 < H < 2$, and definitively heterogeneous if $H \geq 2$.

In conclusion, the purpose of using the homogeneity evaluation is to identify the homogeneous group for different duration in hours for regional quantile estimates. Furthermore, this approach is used to group the observed data into regional sites in which each group has a different duration of precipitation.

3.5.3 Estimating the regional quantile values

The regional quantile values are estimated by using the regional L-moment algorithm (Hosking & Wallis, 1997) tools. The regional L-moment algorithm aims to fit data from sites into homogenous regions with a single frequency distribution. This process is a significant step of the project. Hosking and Wallis (1997) tools take data sites through certain processes starting

with calculating the data screening (as explained in chapter 2) until the quantile values are estimated for different probability distributions. The probability distribution chosen for the quantile estimates is Pearson type III distribution. Then, these values are multiplied by the mean of the singular site. The process of estimating the regional quantile is part of the regional frequency analysis (see chapter 2). The key of the process is Z^{dist} values; these are used as a threshold to determine the goodness-of-fit measure.

Z^{dist} values are defined as the goodness-of-fit measure; its goal is to check whether a distribution fits the data acceptably or not. Goodness-of-fit measure is evaluated by means of Monte Carlo simulation experiments, and the data are simulated from homogenous regions with one of four three-parameter frequency distributions.

If a region is acceptably homogenous, Z^{dist} values must be calculated for all candidate frequency distributions (generalized logistic, generalized extreme value, lognormal, Pearson Type III, and generalized Pareto). The growth curves are the relation between cumulative probability and the value of sample. The growth curves must also be computed for accepted distributions. If the growth curve is equal, any distributions are adequate. If the growth curve is not equal, the data might contain problems such as scarcity of data, which means that two models would display differences which are statistically insignificant but operationally important (Hosking & Wallis, 1997). If the region is not acceptably homogenous, a single distribution will not give a valid fit to data site. In this case, the Kappa and Wakeby distributions are used (Hosking & Wallis, 1997).

Finally, the regional quantile values are computed based on the L-moments algorithms that

require homogeneity measures, identification of homogenous groups, and frequency distribution choice. These are then applied to regional data site. The homogeneity tests and identification of homogenous groups help to determine the goodness-of-fit measure of the frequency distributions; however, they could also be used as key factors in the process of quantile estimation.

3.6 Estimation of uncertainty

As mentioned in chapter 1, uncertainty estimations are used to quantify the uncertainty in precipitation data series can be uncertain. Because urban water systems are exposed to risks of flood hazards and data may lack sufficient climate information, uncertainty estimations are crucial. Thus, statistical approaches are used to estimate uncertainty in data; moreover, the uncertainty estimation methods are premised on a stochastic simulation. For example, in Bayesian inference analysis, the uncertainty is computed based on Bayesian estimates of IDF curves. Monte Carlo simulation is another method that is utilized in the WG model, because it has the capability to consider the correlated data input uncertainties such as depth and duration. Repeated resampling of data series by using Monte Carlo simulation is identifying the variability in the data.

3.6.1 Monte Carlo simulation

Monte Carlo simulation is a stochastic simulation that repeats random variables from specific distribution, and it can be intensively computed for specific complex cases. The WG model basically uses the Monte Carlo simulation to produce the simulated precipitation series. Furthermore, the simulation values can be used to estimate the uncertainty in IDF curves.

Because the WG approach does not require an assumption for a probability distribution, Monte Carlo random variables will be used to resample data. Uncertainty will be represented in the graphical plots, which is called “Box and Whisker plots”. The Box and Whisker plots are compatible with the results of the thesis (WG outputs) to display the uncertainty on IDF curves clearly. Box and Whisker plots contain five components: median, maximum value, minimum value, upper quartile and lower quartile. Furthermore, this plot is defined as a series of large amounts of data in order to clearly identify percentiles of data series. The difference between 75 percent quartile and 25 percent quartile is a measure of the uncertainty, which is called Interquartile Range. In conclusion, the uncertainty estimation methods are stochastic, and can be displayed graphically.

Chapter 4: Case Study Application, Results, and Findings

4.1 Case Study Application

Upper Thames River (UTR) in London Ontario is the proposed study area for the project. UTR has experienced severe flooding and drought over the past decade according to data collected from climate stations and used as input to the WG model.

According to Prodanovic and Simonovic (2006), the area of the basin is 5,825 km^2, and its length is 273 km. This basin is frequently developed, and is facing pressure from population. The watershed of the UTR consists of two main tributaries of the river: north and south. The north branch flows south of Mitchell, St. Mary's to London. The south branch flows through Woodstock to east London. The watershed receives approximately 1,000 mm annual precipitation; however, 60 percent of this is lost by hydrologic abstract such as evaporation and evapotranspiration. Furthermore, UTR has documented historical flooding events over the past 300 years. Each year the occurrence of flooding depends on the weather conditions; for example, flooding was significant and destroyed property in summer 2008. For this study, the climate gauges surrounding the case study location indicate the climate data measurements.

4.2 Data description

The surrounding stations are located within 50 km from London, and include London, Dorchester, Ilderton, St. Thomas, Embro, Foldens, Woodstock, Stratford, and Exeter. These stations were chosen because they are exposed to the same weather conditions as the London site, and are similarly affected (Figure 4-1). Table 4-1 presents the nine sites organized from

nearest to farthest distance from the London site. Figure 4-1 indicates the site locations on a map. The nine sites are located within or close to the UTR basin area and were chosen to apply the regional frequency analysis to estimate the uncertainty.

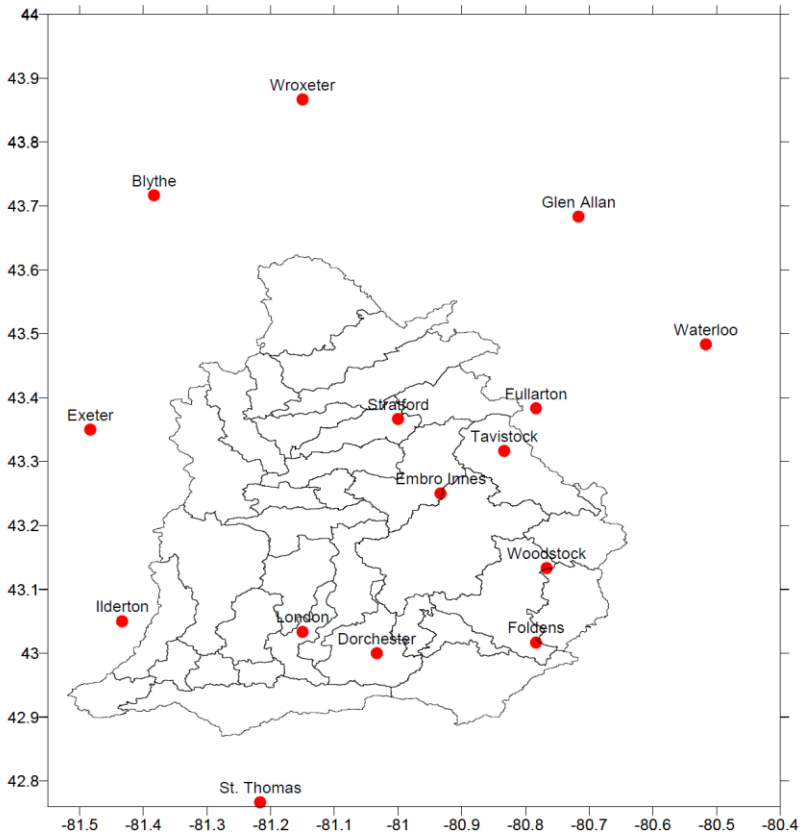

Figure 4-1 Location of case study area. Six stations are located inside border of the basin map (London, Dorchester, Foldens, Woodstock, Stratford and Embro), and three sites are located outside watershed (St. Thomas, Ilderton and Exeter) (adopted from Sharif & Burn, 2007).

Table 4-1 Stations organized by geographical distance from London

Station	Geographical distance from London, ON (km)
London	0
Dorchester	11
Ilderton	24
St. Thomas	30
Embro	31
Foldens	32
Woodstock	34
Stratford	40
Exeter	46

The data were chosen based on several factors, including geographical location (longitude and latitude), distance between stations, and climate data. Although Environment Canada (EC) has many stations, only nine stations were used. The period of historical daily data are between 1964 and 2005 and the hourly precipitation data is between 1965 and 2003. However, five stations (Dorchester, Ilderton, Foldens, Exeter and Embro) have hourly precipitation data between 1985 and 2003; the other stations (London, St. Thomas, Woodstock, and Stratford) have data between 1965 and 2000. In addition, certain stations (Dorchester, Ilderton, Foldens, Exeter, and Embro) are missing IDF data; thus, the missing data **are** computed based on the hourly precipitation. While other stations (London, St. Thomas, Woodstock, and Stratford) have IDF information, these four stations have various ranges of data periods. Specifically, London station has IDF data between 1943 and 2003, St. Thomas station has data between 1926 and 2003,

Woodstock station had data between 1962 and 2003, and Stratford station has data between 1966 and 2003 (Table 4-2). Considering single site quantile values estimates (see Chapter 3), and based on the hourly precipitation data, IDF values are calculated for these missing stations by computing the annual maximum precipitation for each duration, because the IDF values are dependent on annual maximum precipitation.

Table 4-2 Stations used through WG

	IDF data		Daily precipitation		Hourly precipitation	
Station	From	To	From	To	From	To
London	1943	2003	1964	2005	1965	2000
Dorchester	-	-	1964	2005	1985	2003
Ilderton	-	-	1964	2005	1985	2003
St. Thomas	1926	2003	1964	2005	1965	2000
Embro	-	-	1964	2005	1985	2003
Foldens	-	-	1964	2005	1985	2003
Woodstock	1962	2003	1964	2005	1965	2005
Stratford	1966	2003	1964	2005	1965	2000
Exeter	-	-	1964	2005	1985	2003

In addition, the data consists of seven variables which are logged by climate gauges. Variables are maximum temperature, minimum temperature, precipitation, humidity, wind direction, velocity, and radiation. Precipitation is only used for uncertainty estimations. Table 4-3 provides the mean annual precipitation in (mm) for nine stations. The location of each site might affect the reading of the climate data; for example, the highest mean annual precipitation is Stratford, and the lowest value is Woodstock. 5 of 9 sites (Dorchester, Ilderton, Embro, Foldens,

and Exeter) have the same number of observations, because they are computed based on the hourly precipitation data for the same time period. On the other hand, the other sites (London, St. Thomas, Woodstock, and Stratford) are different (Table 4-4), because climate stations have already measured these sites.

Table 4-3 Data for project with mean annual precipitation for each site (Burn & Sharif, 2006)

Stations	Mean annual precipitation (mm)
London	980
Dorchester	1034
Ilderton	1008
St. Thomas	985
Embro	984
Foldens	945
Woodstock	941
Stratford	1056
Exeter	1008

A number of observations are used in the L-moments algorithm to determine the homogenous group. The homogeneity test is required for regionalizing the stations into a group. Each group contains a number of sites, which are estimated based on the homogeneity test results. Because the number of observations and group sites might be associated with uncertainty, regionalization has been utilized. As a result, the regionalization has been determined for durations of 1 hour, 2, 6, 12, and 24 hours. Table 4-5 provides the homogeneity test results for different duration in hours. 5 of 9 sites were grouped together for 1 and 2 hour precipitation events, 4 of 9 sites were grouped together for 6 hour precipitation events, and all 9

sites were grouped together for 12 and 24 hour precipitation events. These site numbers are used to estimate the regional quantile values.

Table 4-4 Number of observations for each site

Site	Number of observations of precipitation
London	27
Dorchester	19
Ilderton	19
St. Thomas	74
Embro	19
Foldens	19
Woodstock	16
Stratford	35
Exeter	19

Table 4-5 Site numbers for different time durations obtained based on the homogeneity test

Duration (hours)	Number of sites	Sites names
1	5	London, Dorchester, Ilderton, St. Thomas and Embro
2	5	
6	4	London, Dorchester, Ilderton, St. Thomas
12	9	London, Dorchester, Ilderton, St. Thomas, Embro, Foldens, Woodstock, Stratford and Exeter
24	9	

To conclude, although the data of UTR includes nine sites, five sites IDF data are missing due to unavailable data records. Calculating the annual maximum precipitation for each duration

period solves the missing data. These data are used through the entire thesis. To complete this information, data from remaining sites were estimated to analyze the IDF values and create their plots. Data records have been regionalized for different durations in order to use regional frequency analysis tools to estimate the regional quantile values. As a result, the homogeneity test has been used to form sites that each measure different durations of precipitation events.

4.3 Plotting Data

The quantile estimates were transferred into precipitation depth by multiplying the depth by the mean of the single site (London, ON see section 4.1). Afterwards, the results were statistically analyzed to obtain the basic statistics of mean, median, standard deviation, etc. for all the runs in respect to the combination of duration and return period. The results were further represented in Box and Whisker plots to illustrate the uncertainty more clearly. Moreover, a comparison was carried out between the analyzed historical data for a single site and the regional simulated data works with the IDF curves. In the main body of this thesis, only certain results will be highlighted (see Tables 4-6 and 4-7).

Three plots have been generated for all results: Intensity-Duration, Depth-Duration, and Depth-Frequency. An example for each plot-type is given in the following sub-sections. Moreover, the results of regional frequency analysis based on L-moments approach are represented in Figures 4-2 to 4-14. These figures indicate the observed single site (London) and the box plots of simulated regional data. The London site and regional sites (grouped sites) are determined by using inverse of Pearson type III distribution.

4.3.1 Intensity-Duration plot

Figures 4-2 to 4-5 illustrate the relationship between duration of storm and intensity, and they are converted to depth duration relation. Each figure represents a different return period in years, and indicates a curve for an observed single site as well as a box plot for regional simulated values. The box plot consists of five components: first quartile (25 percent), median (50 percent), third quartile (75 percent), minimum value, and maximum value. Because of the

relation between the observed single site IDF curves and regional simulated IDF curve, the single site IDF curves fall within the range of the regional simulated IDF curves. The error bars in each plot represent the range of the data, which are between maximum and minimum values. Furthermore, there are two error bars in each plot. The first error bar is called upper bound and the second is called lower bound. To calculate these bounds, the upper bound is the difference between third quartile (75%) and maximum value of the data. Similarly, the lower bound is the difference between first quartile (25%) and minimum value of data range. As a result, the single site curves and regional sites all fall within the same range of data series as shown in all figures in each section.

Intensity is a measure of a storm event over time, and can be obtained by dividing the storm depths by durations. Therefore, the highest intensity for each return period is one hour duration, and the smallest intensity for each return period is 24 hours duration. As mentioned in chapter 3, the difference between upper quartile and the lower quartile is called interquartile range; moreover, this range can be used for uncertainty measure. Each figure displays a different uncertainty value for each return periods and durations. In all figures the uncertainty decreases with increases in the duration of storm. Furthermore, each IDF curve has different uncertainty values for each return period.

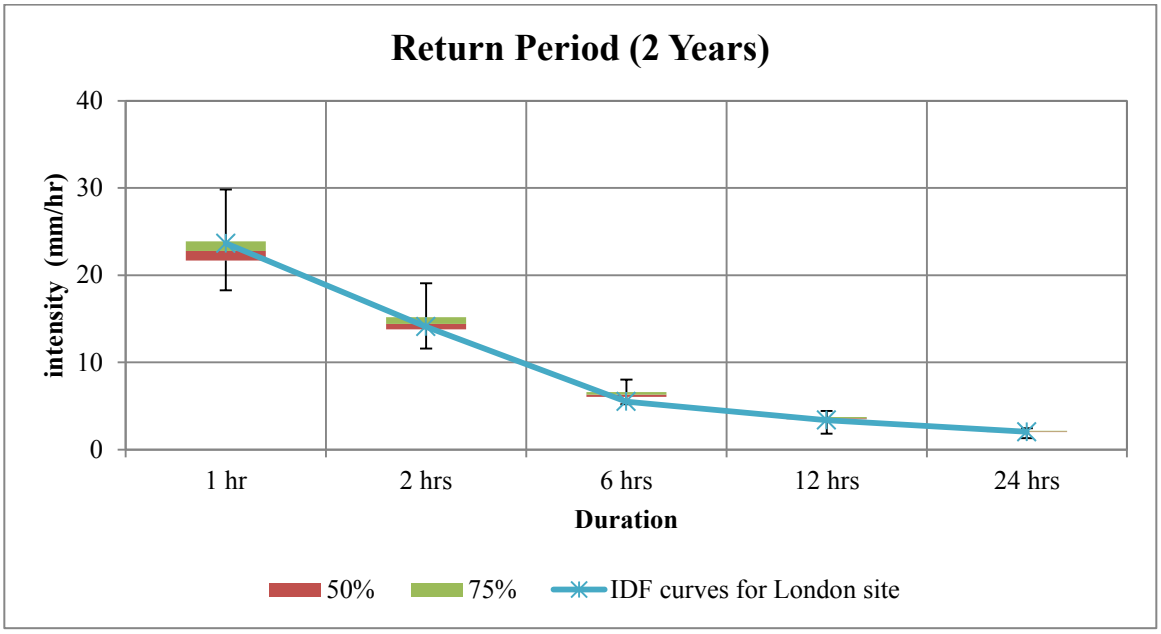

Figure 4-2 IDFs comparison of simulated, historical data for London for return period two years. The box plots are lower quartile (25th percentile), median (50th percentile), and upper quartile (75th percentile).

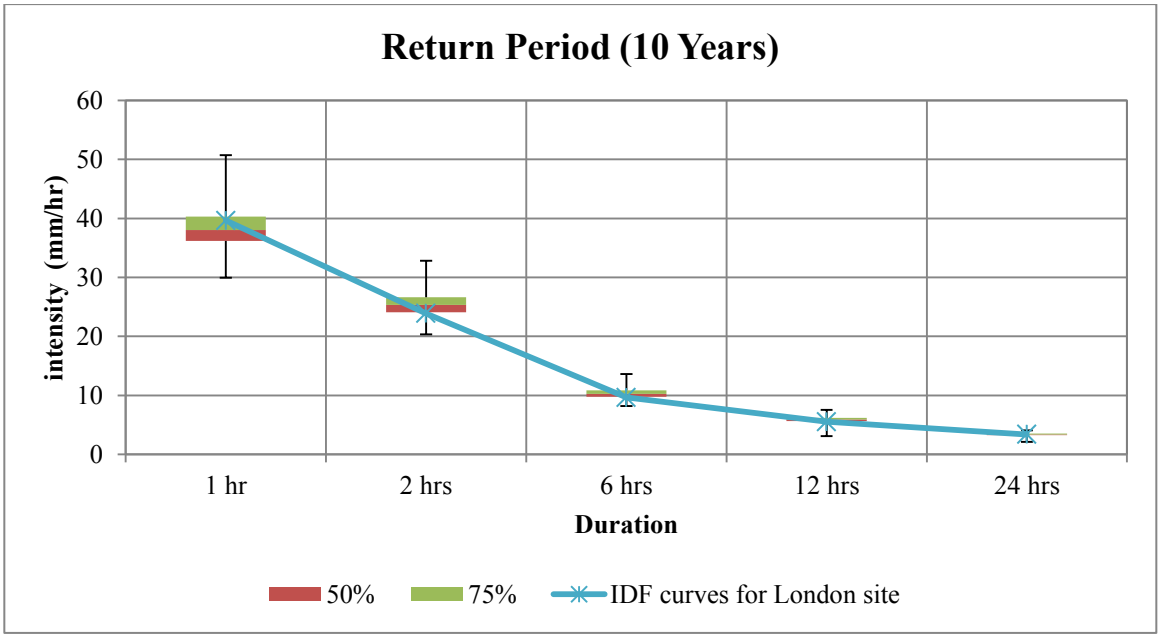

Figure 4-3 IDFs comparison of simulated, historical data for London for return period 10 years. The box plots are lower quartile (25th percentile), median (50th percentile), and upper quartile (75th percentile).

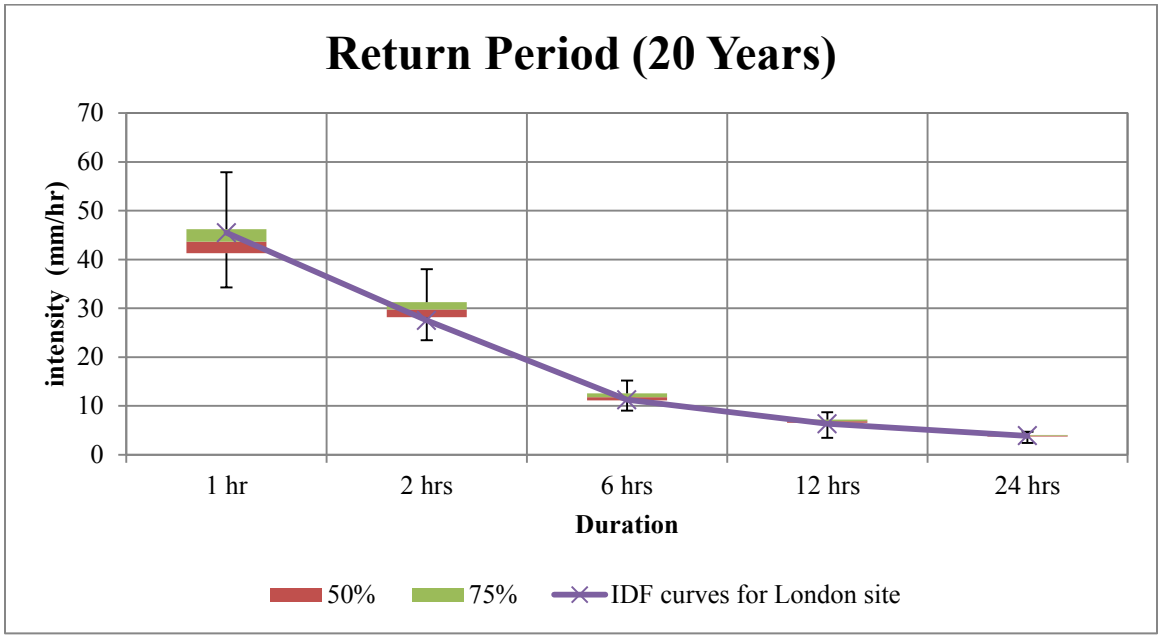

Figure 4-4 IDFs comparison of simulated, historical data for London for return period 20 years. The box plots are lower quartile (25th percentile), median (50th percentile), and upper quartile (75th percentile).

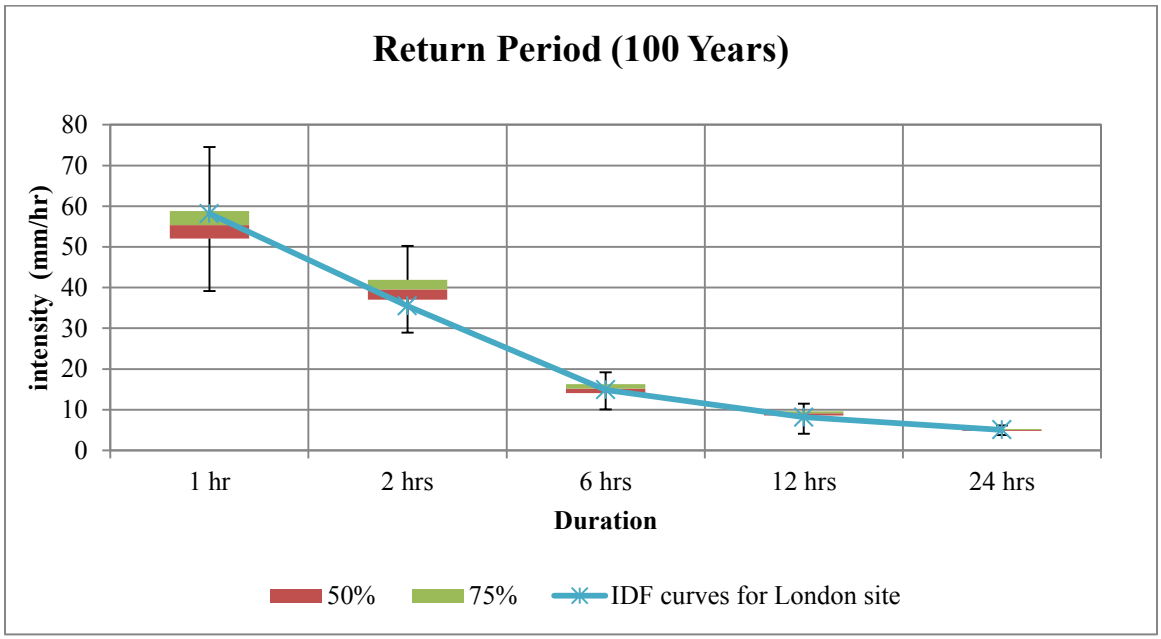

Figure 4-5 IDFs comparison of simulated, historical data for London for return period 100 years. The box plots are lower quartile (25th percentile), median (50th percentile), upper quartile (75th percentile).

4.3.2 Depth-Duration plot

Figures 4-6 to 4-9 indicate relationships between duration of the storm, depth, and frequency called Depth Duration Frequency (DDF) curves. Each figure represents a different return period in years and indicates two curves: the first curve is historical single site data and second curve is regional simulated data. The components of box plots are described in section 4.3.1.

The comparison between the DDF curves for both observed single site (London) and the regional simulated data indicates that historical single site DDF curves fall within the regional simulated DDF curve, because both curves are having same range of the data. For example, in Figure 4-6 the data points of six hours are in the range of simulated DDF curves, because the DDF curves have been regionalized for DDF analysis. Each figure has a different uncertainty value for each return period. In all figures the uncertainty increases with increases in the duration of storm. The smallest uncertainty in all diagrams is one hour duration, and the highest is 24 hours duration. Furthermore, each DDF curve has different uncertainty values for each return period.

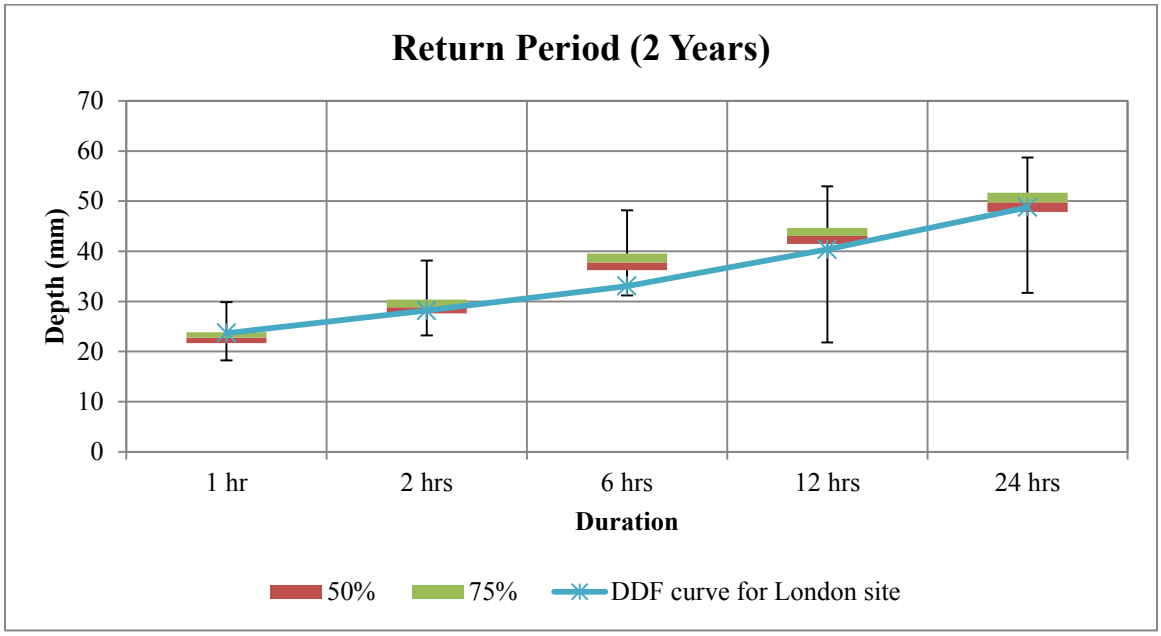

Figure 4-6 DDFs comparison of simulated, historical data for London for return period two years. The box plots are lower quartile (25th percentile), median (50th percentile), and upper quartile (75th percentile).

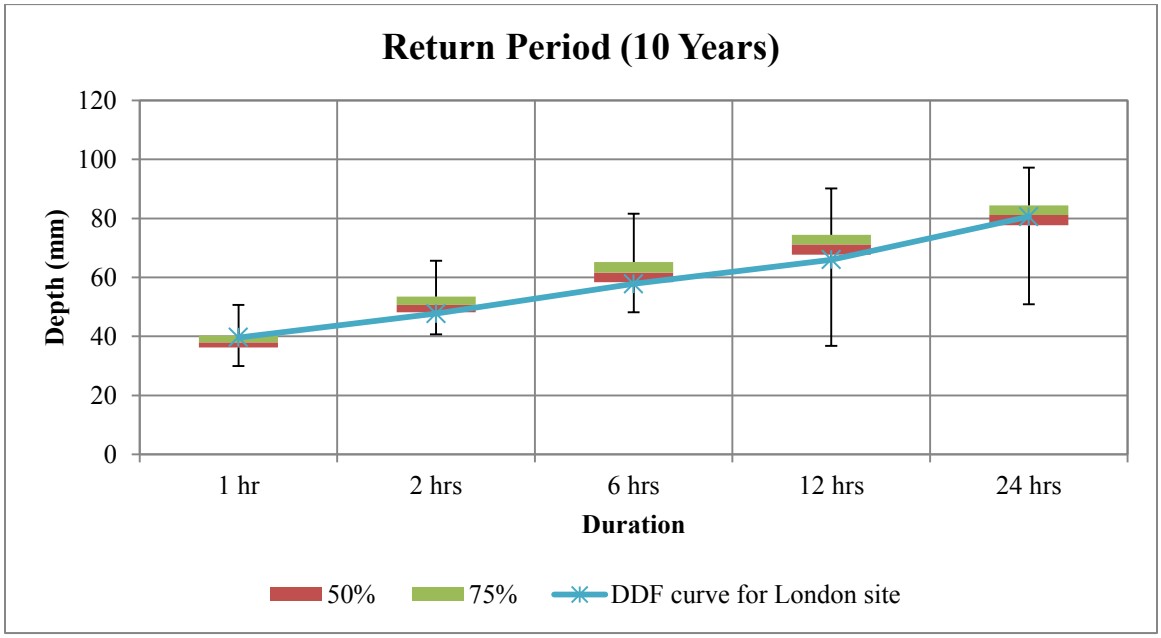

Figure 4-7 DDFs comparison of simulated, historical data for London for return period 10 years. The box plots are lower quartile (25th percentile), median (50th percentile), and upper quartile (75th percentile).

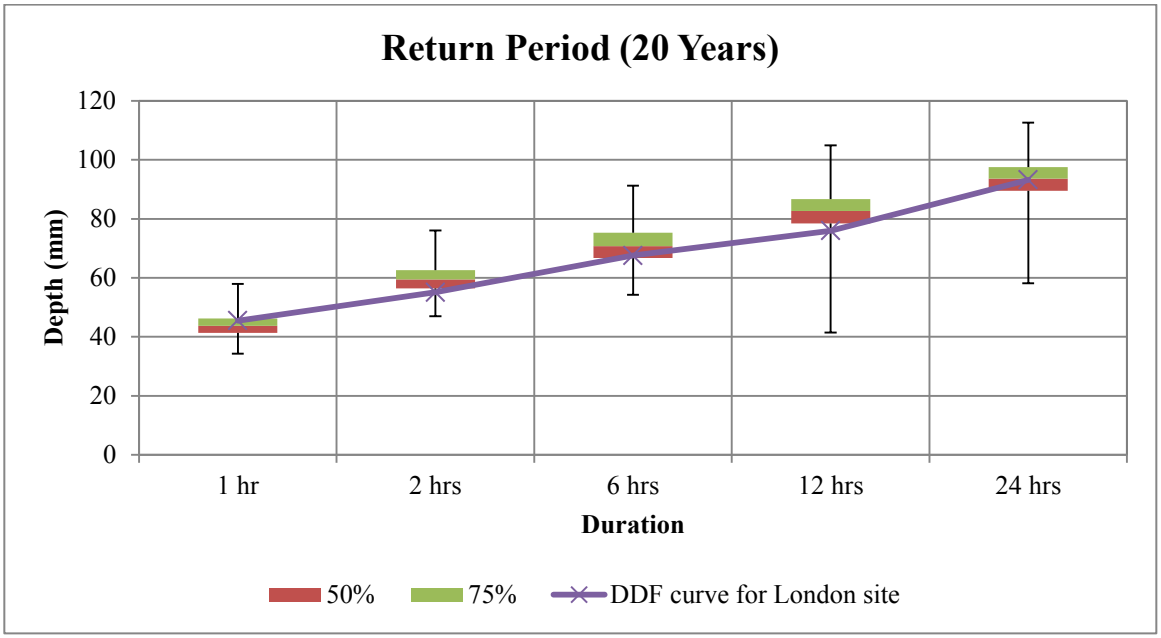

Figure 4-8 DDFs comparison of simulated, historical data for London for return period 20 years. The box plots are lower quartile (25th percentile), median (50th percentile), and upper quartile (75th percentile).

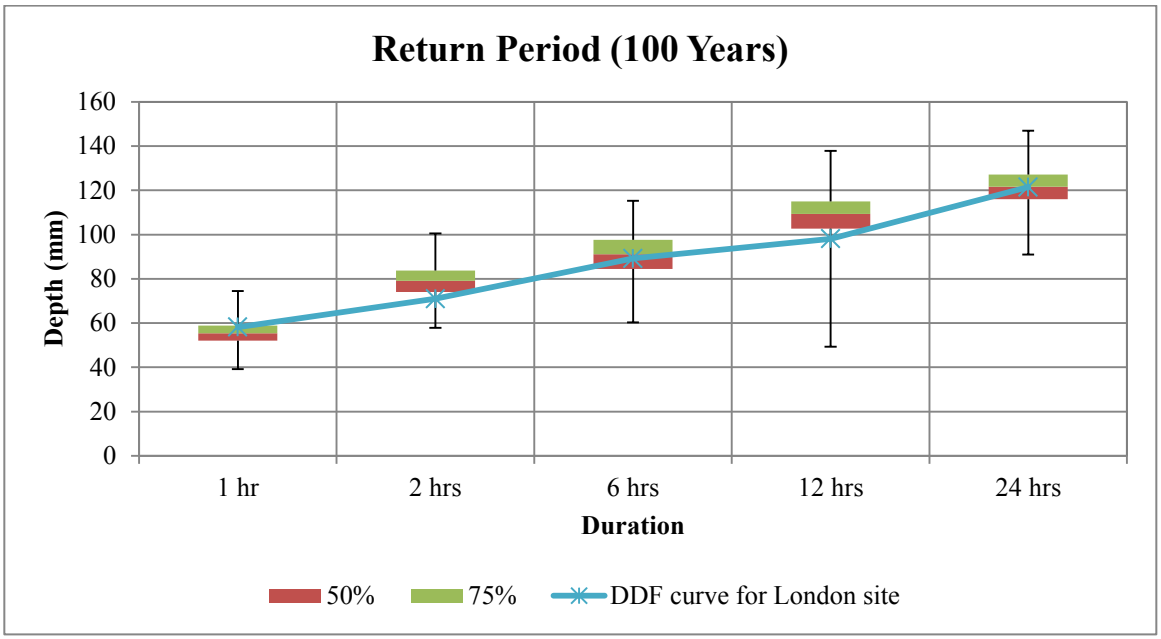

Figure 4-9 DDFs comparison of simulated, historical data for London for return period 100 years. The box plots are lower quartile (25th percentile), median (50th percentile), and upper quartile (75th percentile).

4.3.3 Depth-Frequency plot

Finally, the diagrams in Figures 4-11 to 4-14 illustrate the depth (in millimeters) versus different return periods (in years) for durations of 1, 2, 6, 12, and 24 hours. Analyzed historical single site data falls within the simulated results. However, single historical DDF data obtained for each single site are within the range of DDF data simulated results. Some plots are not 100 percent within range of the simulated DDF, because the historical DDF curves are estimated at-site (Figure 4-13); in addition, the simulated DDF curves have been regionalized for DDF analysis. Each figure illustrates a different uncertainty value for different durations. In all figures the uncertainty increases with increases in the return period, the reason why could be the short record or number of stations.

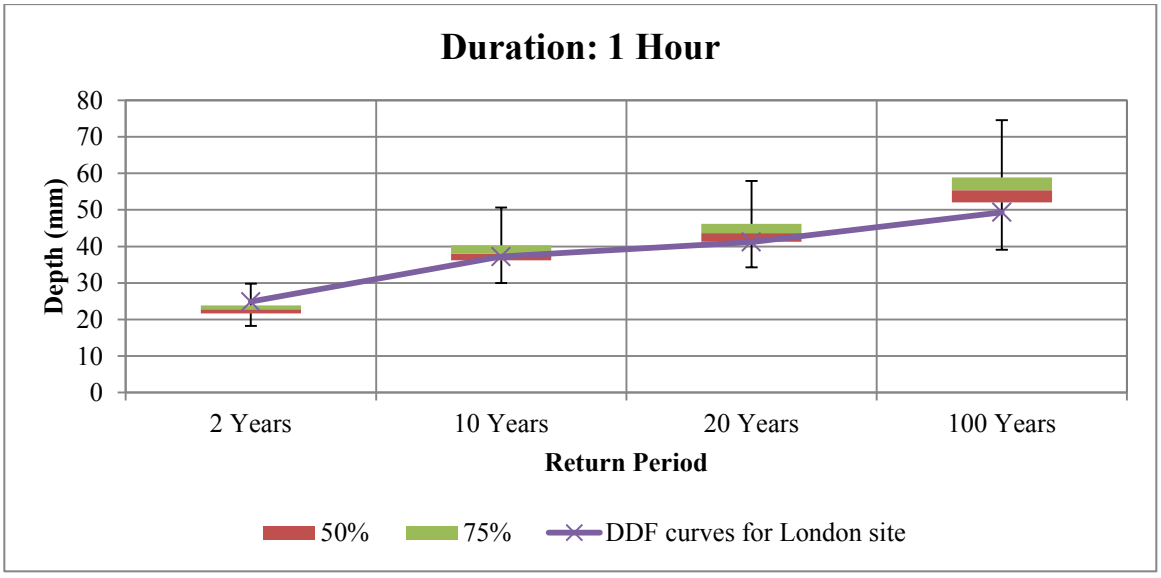

Figure 4-10 DDFs comparison of simulated, historical data for London site for one hour duration. The box plots are lower quartile (25th percentile), median (50th percentile), and upper quartile (75th percentile).

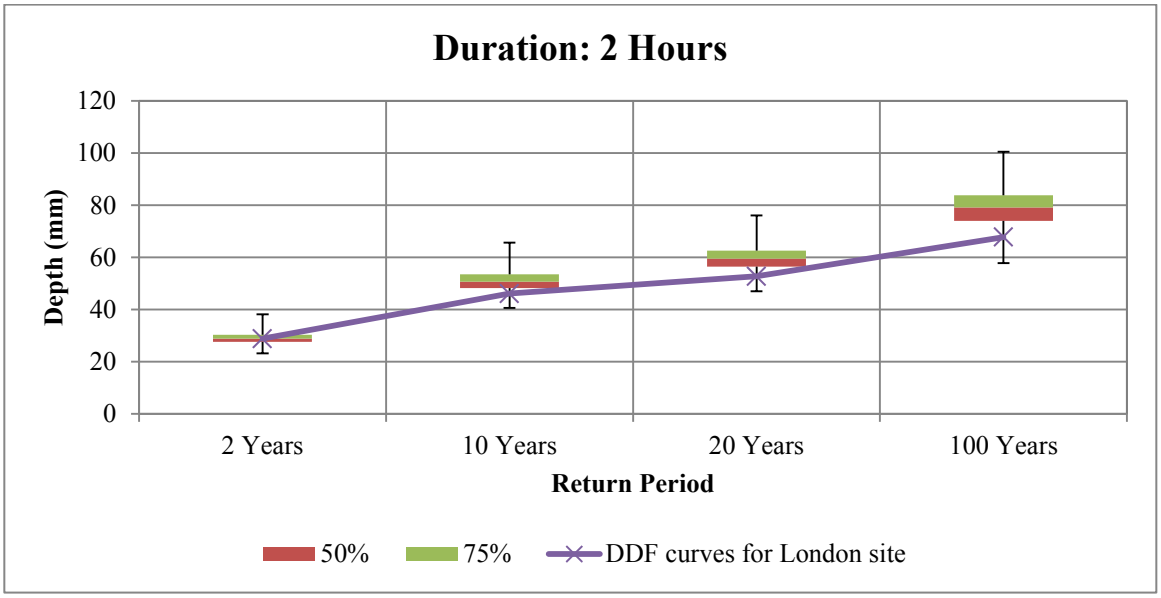

Figure 4-11 DDFs comparison of simulated, historical data for London site for two hours duration. The box plots are lower quartile (25th percentile), median (50th percentile), and upper quartile (75th percentile).

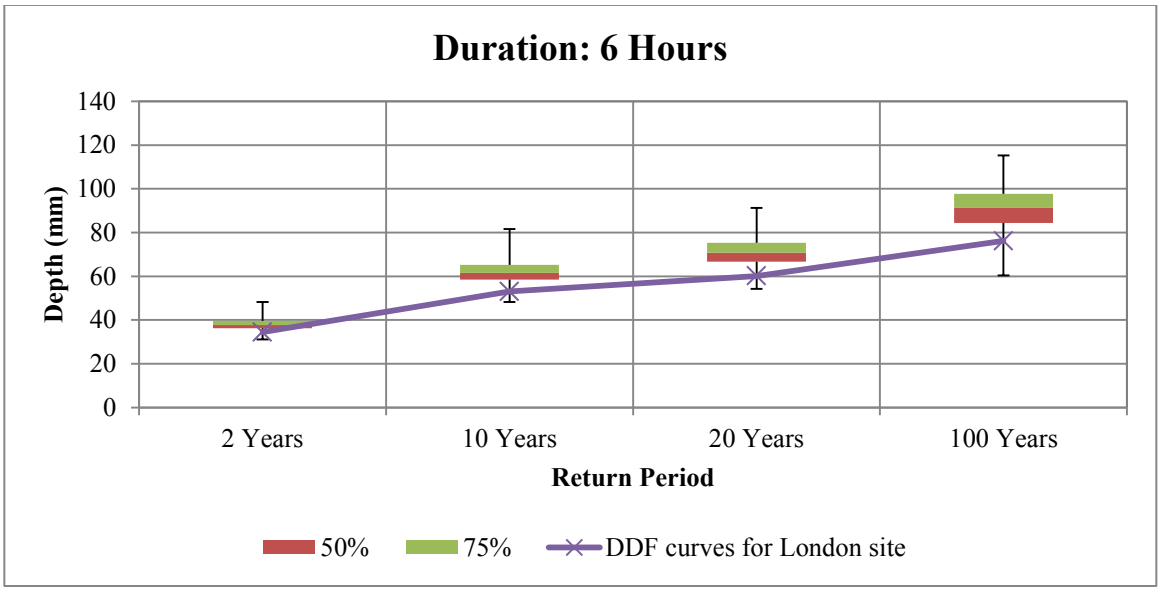

Figure 4-12 DDFs comparison of simulated, historical data for London site for six hours duration. The box plots are lower quartile (25th percentile), median (50th percentile), and upper quartile (75th percentile).

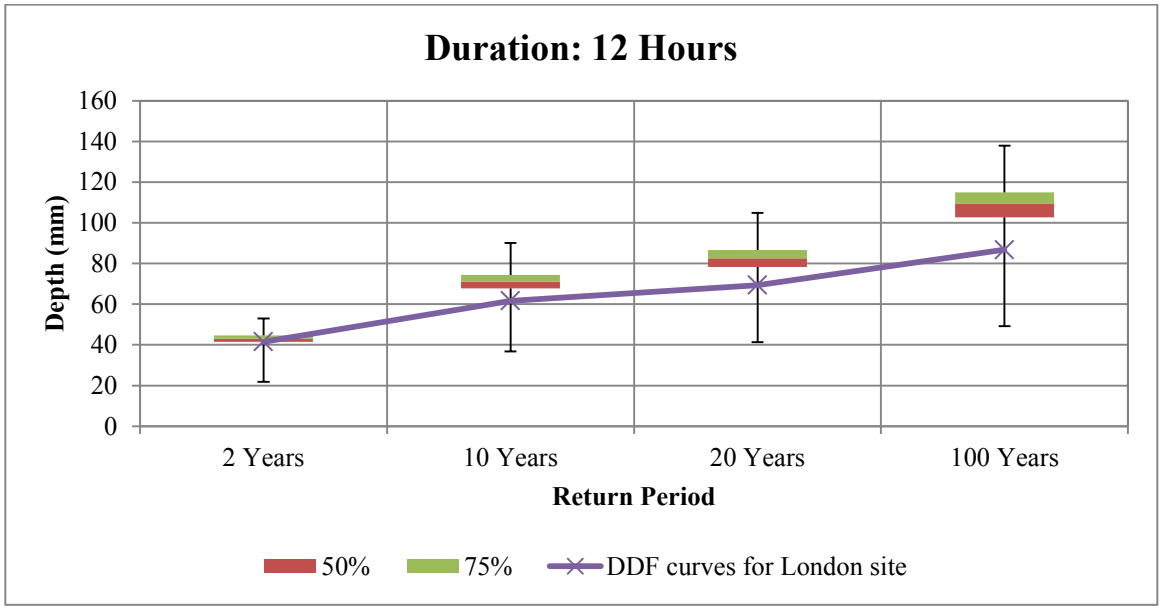

Figure 4-13 DDFs comparison of simulated, historical data for London site for tewelve hours duration. The box plots are lower quartile (25th percentile), median (50th percentile), and upper quartile (75th percentile).

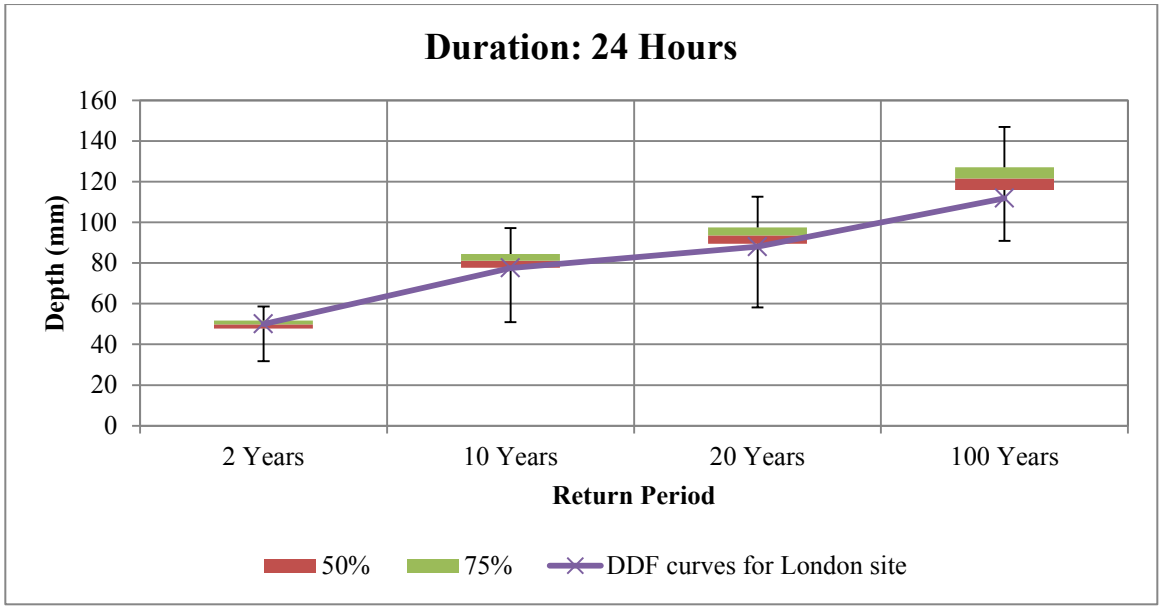

Figure 4-14 DDFs comparison of simulated, historical data for London site for tewenty four hours duration. The box plots are lower quartile (25th percentile), median (50th percentile), and upper quartile (75th percentile).

4.3.4 Depth-Duration results

Table 4-6 presents the analysis for all 1000 simulated runs with respect to different depths and durations for each return period. The examined estimates are precipitation depth measured in (mm).

4.3.5 Depth-Frequency results

Table 4-7 presents the analysis for all 1000 simulated runs with respect to different return periods and durations. The examined estimates are precipitation depths measured in (mm).

4.4 Findings and estimation of the uncertainty summary

The following points outline the main findings after examining the results:

1. From the obtained plots, it is very clear that as the return period and duration increases, the uncertainty, which is the difference between third and first quartile, increases in the plots of depth-duration and depth-frequency. On the other hand, the uncertainty decreases when the return period increases in plots of intensity- frequency.
2. The obtained results suggest that as precipitation duration increases, uncertainty slightly increases (Tables 4-6 and 4-7).
3. The data obtained from the historical single site (London) IDF curves falls within the range of most of the simulated data, thereby ensuring confidence in correctness.
4. As mentioned in the previous section, the difference between median and upper quartile defines the uncertainty. Thus, the highest uncertainty was found in both intensity rate with duration and depth with duration.
5. Previous studies have estimated the uncertainty of the impact of climate change on extreme precipitation. However, this thesis used the Monte Carlo simulation on precipitation data without considering the climate change models. The contribution of this project is to quantify the uncertainty in IDF curves (depth, duration, and frequency).

Table 4-6 Uncertainty analysis for different return periods (All numbers are in mm)

Return Period (2 Years)						Return Period (10 Years)					
Duration	1 hr	2 hrs	6 hrs	12 hrs	24 hrs	Duration	1 hr	2 hrs	6 hrs	12 hrs	24 hrs
Mean	22.84	28.98	37.96	43.15	49.76	Mean	38.27	50.87	61.8	71.11	81.06
SD	1.72	2.03	2.45	2.54	2.87	SD	3.49	3.99	5.07	4.8	5.03
Median	22.79	28.82	37.77	43.07	49.78	Median	38	50.71	61.6	71.13	81.12
Q1	21.67	27.61	36.23	41.49	47.84	Q1	36.19	48.2	58.42	67.73	77.67
Q3	23.88	30.35	39.55	44.66	51.65	Q3	40.27	53.47	65.25	74.39	84.39
Minimum	18.26	23.2	31.18	21.81	31.69	Minimum	29.95	40.67	48.2	36.77	50.86
Maximum	29.83	38.15	48.17	52.95	58.7	Maximum	50.69	65.63	81.62	90.16	97.2
IQR	2.2	2.74	3.33	3.17	3.81	IQR	4.08	5.27	6.83	6.65	6.72
Return Period (20 Years)						**Return Period (100 Years)**					
Duration	1 hr	2 hrs	6 hrs	12 hrs	24 hrs	Duration	1 hr	2 hrs	6 hrs	12 hrs	24 hrs
Mean	43.88	59.6	70.85	82.58	93.47	Mean	55.49	79.23	90.68	109.12	121.54
SD	3.5	4.87	6.23	5.8	5.95	SD	5.15	7.43	9.48	8.98	8.48
Median	43.67	59.46	70.76	82.61	93.59	Median	55.34	79.11	91.16	109.31	121.65
Q1	41.29	56.4	66.7	78.39	89.49	Q1	52.02	74.02	84.42	102.71	115.96
Q3	46.23	62.56	75.29	86.66	97.54	Q3	58.85	83.81	97.63	114.96	127.09
Minimum	34.28	46.96	54.18	41.39	58.09	Minimum	39.13	57.81	60.37	49.24	90.91
Maximum	57.61	76.08	91.26	104.85	112.57	Maximum	74.52	100.49	115.25	137.88	146.99
IQR	4.95	6.15	8.58	8.27	8.05	IQR	6.83	9.79	13.21	12.25	11.13

Table 4-7 Uncertainty analysis for different durations in hours and return periods in years. All numbers are in mm.

1 hr					2 hrs			
Return Period	2 Years	10 Years	20 Years	100 Years	2 Years	10 Years	20 Years	100 Years
Mean	22.84	38.35	43.88	55.49	28.98	50.87	59.60	79.23
SD	1.72	3.04	3.50	5.15	2.03	3.99	4.87	7.42
Median	22.79	38.03	43.67	55.34	28.82	50.71	59.46	79.11
Q1	21.68	36.20	41.28	52.02	27.61	48.21	56.41	74.03
Q3	23.88	40.27	46.22	58.84	30.35	53.48	62.56	83.81
Minimum	18.26	29.95	34.27	39.13	23.20	40.67	46.96	57.81
Maximum	29.83	50.69	57.91	74.52	38.15	65.63	76.08	100.49
IQR	2.19	4.08	4.95	6.83	2.74	5.27	6.15	9.78
6 hrs					**12 hrs**			
Return Period	2 Years	10 Years	20 Years	100 Years	2 Years	10 Years	20 Years	100 Years
Mean	37.96	61.80	70.86	90.70	43.15	71.11	82.58	109.12
SD	2.45	5.07	6.23	9.47	2.54	4.80	5.80	8.97
Median	37.77	61.61	70.76	91.19	43.07	71.13	82.60	109.31
Q1	36.22	58.41	66.73	84.43	41.49	67.73	78.39	102.71
Q3	39.56	65.25	75.29	97.64	44.66	74.39	86.66	114.96
Minimum	31.18	48.20	54.18	60.37	21.81	36.77	41.39	49.24
Maximum	48.17	81.62	91.26	115.25	52.95	90.16	104.85	137.88
IQR	3.34	6.84	8.56	13.21	3.17	6.65	8.27	12.25
24 hrs								
Return Period	2 Years	10 Years	20 Years	100 Years				
Mean	49.76	81.06	93.47	121.54				
SD	2.87	5.03	5.95	8.48				
Median	49.78	81.12	93.59	121.65				
Q1	47.84	77.67	89.49	115.96				
Q3	51.65	84.39	97.54	127.09				
Minimum	31.69	50.86	58.09	90.91				
Maximum	58.70	97.20	112.57	146.99				
IQR	3.81	6.72	8.05	11.13				

Chapter 5: Conclusions and Future Work

5.1 Conclusion

The precipitation records are very important, and they are essential for hydrologic and hydraulic analyses. In this thesis, a process has been used for quantifying uncertainty in IDF curves. The process includes: 1) generating precipitation values with a weather generator model; 2) disaggregating daily data to hourly data; and 3) estimating at-site and pooled extreme precipitation values. The procedure is applicable for both historical data and simulated data. Because the both sites IDF curves fall within same range, the obtained results are reliable and can be helpful for the decision-making process in the design and management of urban water systems e.g., drainage and protection system. Finally, the use of the box plot to illustrate the uncertainty is a simple yet effective approach to identify findings and draw conclusions of different scenarios. The weather generator and Monte Carlo simulations were applied to quantify the uncertainty in IDF curves. Regional frequency analysis process found that Pearson type III distribution (P3) was the most accepted for regional sites. Furthermore, P3 was accepted for all durations (1 hour, 2, 6, 12, and 24 hours) and for all site numbers. Following the steps of regional frequency analysis helps to quantify the uncertainty in IDF curves. In addition, the uncertainty estimation was applied to regional simulated sites, which resulted from WG model.

The results indicated that the uncertainty slightly increases along with increases in duration and return period, and vice versa in the intensity rate with duration for each return period. Increasing the number of simulations and homogenous-pooled sites could quantify the

uncertainty level. In addition, the results show a relationship among single site IDF curves and regional simulated sites.

Currently, the city of London utilizes the IDF curves as standard for design of urban water system and management. Therefore, the IDF curves can be used for designing and management. This would be extremely beneficial because IDF curves identify probability of storm events. This study assessed and compared the current IDF curves with regional IDF curves, quantified understanding of the uncertainty in IDF curves (depth, duration and return period) and found the following results: 1) the uncertainty increased when the durations and return period increased; and 2) dissimilarly, the uncertainty decreased when the durations and return periods increased. 1000 simulations were generated, and the Pearson type III distribution was accepted for most of these simulations. If Pearson type III distribution did not fit, Wakeby distribution was accepted as the alternative. Therefore, the findings of this project will help to develop urban water systems by updating or expanding current systems, for example by changing the size of pipes according to the collected data.

5.2 Future work recommendations

It is recommended that future work focus on programming software that aggregates the different steps into one repository with a single interface. Ideally, the steps should be repeated more than thousands of times and with a larger pool of historical observations in order to estimate the uncertainty in IDF curves. Most research publications have aimed to provide a model that could help determine the impact of climate change on precipitation. For example, Solaiman (2011) found that uncertainty would rise under global warming. The uncertainty

estimation approach introduced in this thesis does not consider uncertainties that arise from using different approaches and parameters such as Monte Carlo simulations (WG) and regional frequency analysis based on L-moment approach. Therefore, future research could involve the uncertainty investigation in the quantification of the uncertainty estimation approach.

References

Al-Dokhayel, A. (1986). Regional rainfall frequency analysis for Qasim. B.S. Project, Civil Engineering Department, King Saud University, Riyadh (K.S.A).

AlHassoun, S. A. (2011). Developing an empirical formulae to estimate rainfall intensity in Riyadh region, King Saud University. *Engineering Sciences, 23*(2), 81-88.

Awadallah, A. G., Elgamal, M., & Elmostafa, A. (2011). Developing intensity-duration-frequency curves in scarce data region: An approach using regional analysis and satellite data, *Scientific Research Publishing, 3*(3), 215-226.

Burn, D. H. (1988). Delineation of groups for regional flood frequency analysis. *Journal of Hydrology, 104*(1–4), 345-361.

Burn, D. H. (1990). Evaluation of regional flood frequency analysis with a region of influence approach. *Water Resources Research, 26*(10), 2257-2265.

Burn, D. H. (1997). Catchment similarity for regional flood frequency analysis using seasonality measures. *Journal of Hydrology, 202*(1–4), 212-230.

Burn, D. H., & Goel, N. K. (2000). The formation of groups for regional flood frequency analysis. Hydrological Sciences Journal, 45(1), 97-112.

Burn, D. H. (2003). The use of resampling for estimating confidence intervals for single site and pooled frequency analysis. *Hydrological Sciences Journal/Journal des Sciences Hydrologiques, 48*(1), 25-38.

Castellarin, A., Burn, D. H., & Brath, A. (2008). Homogeneity testing: How homogeneous do heterogeneous cross-correlated regions seem? *Journal of Hydrology, 360*(1–4), 67-76.

Chow, V. T. (1984). *Handbook of applied hydrology: A compendium of water-resources technology.* New York: McGraw-Hill Book Co.

Chowdhury, J., & Stedinger, J. (1991). Confidence interval for design floods with estimated skew coefficient. *Journal of Hydraulic Engineering, 117*(7), 811-831.

Chowdhury, J. U., Stedinger, J. R., & Lu, L.-H. (1991). Goodness-of-fit tests for regional generalized extreme value flood distributions. *Water Resources Research, 27*(7), 1765-1776.

Coles, S. (2001). An introduction to statistical modeling of extreme values: Springer series in statistics: Springer.

Coles, S., Pericchi, L. R., & Sisson, S. (2003). A fully probabilistic approach to extreme rainfall modeling. *Journal of Hydrology, 273*(1–4), 35-50.

DeCoursey, D. G., (1973). Objective Regionalization of Peak Flow Rates. In: Floods and Droughts, E. F.Koelzer, V. A.Koelzer, and K.Mahmood (Editors) Proceedings of the Second International Symposium in Hydrology, September 11-–13, 1972, *Fort Collins, Colorado. Water Resources Publications, Fort Collins , Colorado , pp. 395405.*

Dodangeh, E., Shao, Y., & Daghestani, M. (2012). L-Moments and fuzzy cluster analysis of dust storm frequencies in Iran. *Aeolian Research, 5*(0), 91-99.

Drees, H., & Kaufmann, E. (1998). Selecting the optimal sample fraction in univariate extreme value estimation. *Stochastic Processes and their Applications, 75*(2), 149-172.

Dupont, B. S., & Allen, D. L. (2000). Revision of the rainfall intensity duration curves for the commonwealth of Kentucky. Retrieved 01/02, 2013 from http://www.ktc.uky.edu/projects/revision-of-the-rainfall-intensity-duration-curves-for-the-commonwealth-of-kentucky/

Durbin, J., & Knott, M. (1972). Components of Cramér-von Mises statistics. .*Journal of the Royal Statistical Society*, B, 290-307.

Eslamian, S. S., & Feizi, H. (2007). Maximum monthly rainfall analysis using L-moments for an arid region in Isfahan province, Iran. *Journal of Applied Meteorology and Climatology, 46*(4), 494-503.

Fill, H. D., & Stedinger, J. R. (1995). Homogeneity tests based upon Gumbel distribution and a critical appraisal of Dalrymple's test. *Journal of Hydrology, 166*(1–2), 81-105.

Fowler, H. J., & Kilsby, C. G. (2003). A regional frequency analysis of United Kingdom extreme rainfall from 1961 to 2000. *International Journal of Climatology*, *23*(11), 1313-1334.

Ghosh, S., & Mujumdar, P. P. (2007). Nonparametric methods for modeling GCM and scenario uncertainty in drought assessment. *Water Resources Research, 43*(7).

Greenwood, J. A., Landwehr, J. M., Matalas, N. C., & Wallis, J. R. (1979). Probability weighted moments: Definition and relation to parameters of several distributions expressible in inverse form. *Water Resources Research, 15*(5), 1049-1054.

Grimaldi, S., Kao, S. C., Castellarin, A., Papalexiou, S. M., Viglione, A., Laio, F., & Gedikli, A. (2011). 2.18 - Statistical Hydrology. In W. Peter (Ed.), *Treatise on Water Science* (pp. 479-517). Oxford: Elsevier.

Gubareva, T., Gartsman, B. (2010). Estimating distribution parameters of extreme hydrometeorological characteristics by L-moments method. *Water Resources, 37*(4), 437-445.

Guo, S., & Ying, A. (1997). Uncertainty analysis of impact of climate change on hydrology and water resources. *IAHS Publications-Series of Proceedings and Reports-Intern Assoc Hydrological Sciences*, *240*, 331-338.

Hailegeorgis, T., & Burn, D. H., (2009). Uncertainty assessment of the Impacts of climate change on extreme precipitation events. Retrieved 12/04/2012 from http://www.eng.uwo.ca/research/iclr/fids/publications/cfcas quantifying_uncertainty/Reports/Teklu_report.pdf

Hosking, J., & Wallis, J. (1993). Some statistics useful in regional frequency analysis. *Water Resources Research*, *29*(2), 271-281.

Hosking, J., Wallis, J. R., & Wood, E. (1985). Estimation of the generalized extreme-value distribution by the method of probability-weighted moments. *Technometrics, 27*(3), 251-261.

Hosking, J. R. M. (1990). L-moments: Analysis and estimation of distributions using linear combinations of order statistics. *Journal of the Royal Statistical Society*, B,105-124.

Hosking, J. R. M., & Wallis, J. R. (1987). Parameter and quantile estimation for the generalized Pareto distribution. *Technometrics, 29*(3), 339-349.

Hosking, J. R. M., & Wallis, J. R. (1997). *Regional frequency analysis.* Cambridge, UK: Cambridge University Press.

Huard, D., Mailhot, A., & Duchesne, S. (2010). Bayesian estimation of intensity–duration–frequency curves and of the return period associated to a given rainfall event. *Stochastic Environmental Research and Risk Assessment, 24*(3), 337-347.

Ilona, V., Francés, F. 2002. Rainfall analysis and regionalization computing intensity–duration–frequency curves, Universidad Politecnica de Valencia – Departamento de Ingenieria Hidraulica Medio Ambiente – APDO. 22012 – 46071 Valencia – Spain.

Katz, R. W., Parlange, M. B., & Naveau, P. (2002). Statistics of extremes in hydrology. *Advances in Water Resources, 25*(8–12), 1287-1304.

Lian, G. S. (1995). Impact of climatic change on hydrological balance and water resource systems in the Dongjiang Basin, China. *IAHS Publications-Series of Proceedings and Reports-Intern Assoc Hydrological Sciences, 231*, 141-150.

Lin, G. F., & Chen, L. H. (2006). Identification of homogeneous regions for regional frequency analysis using the self-organizing map. *Journal of Hydrology, 324*(1–4), 1-9.

Madsen, H., Rasmussen, P. F., & Rosbjerg, D. (1997). Comparison of annual maximum series and partial duration series methods for modeling extreme hydrologic events: 1. At-site modeling. *Water Resources Research, 33*(4), 747-757.

Mansour, R., & Burn, D. H., (2010). Weather generator and hourly disaggregation model. Retrieved 12/07/2012 from http://www.eng.uwo.ca/research/iclr/fids/publications/cfcas-quantifying_uncertainty/Reports/WG_Report.pdf

Markus, M., Angel, J. R., Yang, L., & Hejazi, M. I. (2007). Changing estimates of design precipitation in Northeastern Illinois: Comparison between different sources and sensitivity analysis. *Journal of Hydrology, 347*(1–2), 211-222.

Melching, C. S., Yen, B. C., & Wenzel, H. G. (1990). A reliability estimation in modeling watershed runoff with uncertainties. *Water Resources Research, 26*(10), 2275-2286.

Norbiato, D., Borga, M., Sangati, M., & Zanon, F. (2007). Regional frequency analysis of extreme precipitation in the eastern Italian Alps and the August 29, 2003 flash flood. *Journal of Hydrology, 345*(3–4), 149-166.

Núñez, J. H., Verbist, K., Wallis, J. R., Schaefer, M. G., Morales, L., & Cornelis, W. M. (2011). Regional frequency analysis for mapping drought events in north-central Chile. *Journal of Hydrology, 405*(3–4), 352-366.

Overeem, A., Buishand, A., & Holleman, I. (2008). Rainfall depth-duration-frequency curves and their uncertainties. *Journal of Hydrology, 348*(1–2), 124-134.

Pilon, P. J., & Adamowski, K. (1992). The value of regional information to flood frequency analysis using the method of L-moments. *Canadian Journal of Civil Engineering, 19*(1), 137-147.

Prodanovic, P., & Simonovic, S. P. (2007). Development of rainfall intensity duration frequency curves for the City of London under the changing climate. Retrieved 12/07/2012 from http://www.eng.uwo.ca/research/iclr/fids/publications/products/58.pdf

Prudhomme, C., Jakob, D., & Svensson, C. (2003). Uncertainty and climate change impact on the flood regime of small UK catchments. *Journal of Hydrology, 277*(1–2), 1-23.

Scholz, F. W., & Stephens, M. A. (1987). K-sample Anderson–Darling tests. Journal of the American Statistical Association, 82(399), 918-924.

Sharif, M., & Burn, D. H. (2006). Simulating climate change scenarios using an improved K-nearest neighbor model. *Journal of Hydrology, 325*(1–4), 179-196.

Sharif, M., & Burn, D. (2007). Improved -K nearest neighbor weather generating model. *Journal of Hydrologic Engineering, 12*(1), 42-51.

Sharma, A., Tarboton, D. G., & Lall, U. (1997). Streamflow simulation: A nonparametric approach. *Water Resources Research, 33*(2), 291-308.

Shrestha, R. R., & Simonovic, S. P. (2009). A fuzzy set theory based methodology for analysis of uncertainties in stage-discharge measurements and rating curve. Department of Civil and Environmental Engineering, The University of Western Ontario.

Solaiman, T. A. (2011). Uncertainty estimation of extreme precipitations under climate change: A non-parametric approach (Doctor of Philosophy), University of Western Ontario, London, Ontario, Canada.

Solaiman, T. A., King, L. M., & Simonovic, S. P. (2011). Extreme precipitation vulnerability in the Upper Thames River basin: Uncertainty in climate model projections. *International Journal of Climatology, 31*(15), 2350-2364.

Tebaldi, C., Smith, R. L., Nychka, D., & Mearns, L. O. (2005). Quantifying uncertainty in projections of regional climate change: A Bayesian approach to the analysis of multimodal ensembles. *Journal of Climate, 18*(10), 1524-1540.

U.S water resources council (1976). Guideline for Determining Flood Flow Frequency. Bulleting 17, Hydrology Committee, Washington, D.C.

Vogel, R. W., & McMartin, D. E. (1991). Probability plot goodness-of-fit and skewness estimation procedures for the Pearson Type 3 distribution. *Water Resources Research, 27*(12), 3149-3158.

Vucetic, D., & Simonovic, S. P. (2011). Water Resources Decision Making Under Uncertainty. Department of Civil and Environmental Engineering, The University of Western Ontario.

Xu, Y.-P., Booij, M., & Tong, Y.-B. (2010). Uncertainty analysis in statistical modeling of extreme hydrological events. *Stochastic Environmental Research and Risk Assessment, 24*(5), 567-578.

Yang, T., Shao, Q., Hao, Z.-C., Chen, X., Zhang, Z., Xu, C.-Y., & Sun, L. (2010). Regional frequency analysis and spatio-temporal pattern characterization of rainfall extremes in the Pearl River Basin, China. *Journal of Hydrology, 380*(3–4), 386-405.

Yue-Ping Xu, M. J. B., & Yang-Bin, T. (2010). Uncertainty analysis in statistical modeling of extreme hydrological events. *Stochastic Environmental Research and Risk Assessment, 24*(5), 567-578.

Zadeh, L.A. (1965). Fuzzy sets. Information and control, 8. Retrieved on 10/07/2013 from http://www.bisc.cs.berkeley.edu/Zadeh-1965.pdf